# The Effect of Hyaluronic Acid Coating on Transfection Efficiency and Cytotoxicity of mRNA-Delivering Lipid Nanoparticles on Primary T-cells for CAR T-cell Generation

Hanneke Rijssemus

Universiteit Utrecht

UNIVERSITEIT GENT

# The Effect of Hyaluronic Acid Coating on Transfection Efficiency and Cytotoxicity of mRNA-Delivering Lipid Nanoparticles on Primary T-cells for CAR T-cell Generation

Minor Research Internship | Written Report

Ghent University | Laboratory of General Biochemistry and Physical Pharmacy

May-November 2023

Hanneke Rijssemus
6127495
Drug Innovation
Utrecht University

Supervisors:
Daily supervisor: Laure Harinck
Examiner: Prof. Dr. Raymond Schiffelers
Second examiner: Prof. Dr. Koen Raemdonck

Image source: Inclusion of lipid nanoparticles in skin care products | In-cosmetics connect.

# Table of Contents

## Layman's Summary

Chimeric Antigen Receptor (CAR) T-cell therapy is a treatment that can be used against several types of cancer. In this treatment, the T-cells of the patients, which are a type of immune cells, are taken from their blood, and a CAR is added to the T-cells. The CAR is a receptor that can bind to cancer cells, which allows the CAR T-cells to recognise the cancer cells and kill them. At the moment, the CAR is added to the T-cells with a virus. This can cause some side-effects, is expensive, and takes a long time. One way to solve this is to switch to adding the CAR as mRNA instead of a virus. mRNA can be delivered to the T-cells packaged into small particles called lipid nanoparticles (LNPs). Unfortunately, T-cells do not easily take up these LNPs, which makes it hard to get enough CAR mRNA into the cells. Something is needed to increase the amount of LNPs taken up by T-cells. CD44 is a receptor that is present on the surface of T-cells. By making the LNPs bind to this protein, we expect that more LNPs could be taken up by the T-cells. Hyaluronic acid (HA) is a negatively charged molecule that can bind to CD44. We tested the delivery of mRNA to T-cells with positively charged LNPs that were coated with the negatively charged HA. Strangely, the delivery of mRNA was only lower when the LNPs were coated with HA. After several experiments to discover why, we found the negative charge of HA to be the problem. The charge of the cell membrane is negative, which means that a positively charged LNP will interact with the membrane strongly. When HA blocks the positive charge of the LNP and makes it negative, this interaction is gone, making it harder for the cell to take up the LNP. We tried the coating on an LNP with another composition, which had a neutral charge. With this LNP, the delivery of mRNA did not go lower after HA coating, but also did not go higher. This is probably because beside the HA coating on the LNP, there is also a lot of free HA present. If the free HA already binds to CD44, the HA on the LNP cannot bind to it anymore. With these experiments, we gained valuable information on the different aspects that can prevent a beneficial effect of HA coating. This information can be used to make better working HA-LNPs in the future, so that a better method of making CAR T-cells can be developed.

# Abstract

Chimeric antigen receptor (CAR) T-cell therapy is a cancer therapy in which a patient's own T-cells are engineered to express the chimeric antigen receptor, with which they can recognise and kill cancer cells. The therapy is extremely successful in B-cell cancers, but has some disadvantages as well. Currently, CAR T-cells are produced using viral vectors. Viral vectors integrate the CAR construct in the host DNA, resulting in permanent CAR expression, which can contribute to side-effects like B-cell aplasia, cytokine release syndrome, and insertional mutagenesis. In addition to side-effects, viral vectors are expensive and have a long production process, raising both the costs and time of CAR T-cell therapy. As an alternative, CAR mRNA can be used for safer, cheaper and faster CAR T-cell generation. To avoid the use of viral vectors, non-viral delivery strategies, such as lipid nanoparticles, can be explored to deliver the RNA or other cargo molecules into the T-cells. Since T-cells are resistant to chemical transfection, research is needed to improve transfection of T-cells with LNPs. CD44, a receptor involved in adhesion and migration, is expressed on both inactive and active T-cells and could be targeted to improve transfection. The anionic polymer hyaluronic acid (HA) is the main ligand of CD44. Here, we explore electrostatic coating of HA on cationic LNPs to improve the delivery of mRNA to primary T-cells. After HA coating, the transfection of primary T-cells by the cationic LNPs decreased instead of increasing. Parameters such as interference from PEGylated lipids, HA-CD44 binding on T-cells, and stability of HA coating were tested to rule out their role in the decrease of transfection efficiency. Coating with an alternative anionic polymer without CD44-affinity showed that the charge switch from cationic to anionic is most likely responsible for the decrease in transfection. HA coating on neutral LNPs did not decrease transfection, but neither did it increase. It is hypothesised that an excess of free HA present in the solution after coating is blocking the HA coated LNPs from binding to CD44. To conclude, we did not improve transfection of primary T-cells. However, we provided valuable information into factors influencing the effect of HA coating. In the future, this information can help to develop successful HA-coated LNPs for T-cell transfection and contribute to the development of safer and more accessible CAR T-cell therapy.

# 1 Introduction

During recent years cancer treatment has been revolutionised by immunotherapies, such as immune checkpoint inhibitors, tumour vaccines, and adoptive cell therapy (ACT).[1] In ACT, the patient's own immune cells are collected and engineered to kill pathogens or cancer cells. The three main ACTs are tumour-infiltrating lymphocyte therapy, engineered T-cell receptor T-cell therapy, and chimeric antigen receptor (CAR) T-cell therapy, of which CAR T-cell therapy is currently the most advanced and successful.[1] In CAR T-cell therapy, the T-cells are genetically engineered to express chimeric receptors.[2] The chimeric receptor, or CAR, consists of an extracellular domain that can recognise and bind to an antigen presented on cancerous cells, and an intracellular domain that activates the T-cell upon antigen binding to the receptor. Consequently, the CAR T-cells are able to bind to the cancer cells and destroy them.[2] The first CAR T-cell therapy, Kymriah®, was approved in 2017 by the FDA for the treatment of B-cell precursor acute lymphoblastic leukaemia (ALL).[3] The CAR construct in Kymriah® recognises the well-known B-cell marker CD19, causing the engineered T-cells to bind and destroy the cancerous B-cells.[3] Since then, five other CAR T-cell therapies have been approved, all targeting either CD19 or B-cell maturation antigen (BCMA) on B-cells in various haematological tumours (*Tab. 1*).[4] In solid tumours, CAR T-cell therapy has not yet been successful for a variety of reasons, including the lack of a suitable tumour-specific antigens and an inability to penetrate deeply into the tumour tissue. Nevertheless, the efficacy in haematological B-cell tumours is very high, with response rates of 70-90%.[5,6]

***Table 1.*** *Overview of CAR T-cell therapies currently approved by the FDA and EMA.*[7-12]

| CAR T-cell therapy | Target | Indications | Vector |
|---|---|---|---|
| **Kymriah**<br>*Tisagenlecleucel* | CD19 | B-cell Acute Lymphoblastic Leukaemia<br>Diffuse Large B-cell Lymphoma<br>Follicular Lymphoma | Lentivirus |
| **Yescarta**<br>*Axicabtagene Ciloleucel* | CD19 | Diffuse Large B-cell Lymphoma<br>High-grade B-cell lymphoma<br>Follicular Lymphoma | Retrovirus |
| **Tecartus**<br>*Brexucabtagene Autoleucel* | CD19 | B-cell Acute Lymphoblastic Leukaemia<br>Mantle Cell lymphoma | Retrovirus |
| **Abecma**<br>*Idecabtagene Vicleucel* | BCMA | Multiple Myeloma | Lentivirus |
| **Carvykti**<br>*Ciltacabtagene Autoleucel* | BCMA | Multiple Myeloma | Lentivirus |
| **Breyanzi**<br>*Lisocabtagene Maraleucel* | CD19 | Diffuse Large B-cell Lymphoma<br>High-Grade B-cell Lymphoma<br>Follicular Lymphoma | Lentivirus |

Unfortunately, the therapy has several risks as well. During the production process of CAR T-cells, T-cells are isolated from the patients via leukapheresis, transduced with a vector containing the genetic information for the CAR construct, and expanded to sufficient numbers before infusion back into the patient. All CAR T-cell therapies currently approved use either a lentiviral or retroviral vector for transduction (*Tab. 1*), which contributes to many of the risks associated with CAR T-cell therapy.[7-12] Retro- and lentiviruses are RNA viruses that transcribe their RNA content into DNA using viral reverse transcriptase, and integrate it into the host genome.[13] This will lead to a permanent CAR expression in the cells and its descendants as it proliferates. The engineered CAR T-cells target cancerous B-cells via CD19 or BCMA, which are antigens expressed on both malignant and healthy B-cells. Hence, the stable CAR expression can lead to chronically low B-cell counts, a condition known as B-cell aplasia.[14] This consequently causes hypogammaglobulinemia, a lack of gamma immunoglobulins (IgG) in the blood, which leads to increased susceptibility to infection-related morbidity.[14] Hypogammaglobulinemia can

be treated via IgG substitution therapy. However, potentially lifelong intravenous or subcutaneous IgG injections are required, which can greatly impact the patient's life.[14]

Another common complication of CAR T-cell therapy is cytokine release syndrome (CRS). CRS is a systemic inflammatory response that can cause a wide variety of symptoms, including fever, headache, rash, hypotension, shock, vascular leakage, and multi-organ system failure.[15] It occurs in various grades of severity, ranging from mild to severe and life-threatening.[15] CRS is induced by the binding of the CAR to its antigen and consequent activation of bystander immune cells. This activation results in a storm of cytokines being released, which cause systemic inflammation and the subsequent damage.[16] Unfortunately, CRS occurs frequently. A recent systematic review showed CRS occurred in 42-100% of patients participating in various CAR T-cell therapy trials, with 0-46% of these qualifying as severe.[16] Although CRS can be treated with immunosuppressants, this is accompanied by an increased risk of infections.[15] Risk of CRS is highest in the first two weeks post-infusion of the CAR T-cells. However, as virally transfected CAR T-cells persist in the circulation for much longer than two weeks, the risk for CRS extends for a substantially longer period as well. In addition to the on-target immune activation that leads to CRS, the use of viral transduction can lead to the presence of residual viral proteins. While it has never been proven, these viral proteins could theoretically contribute to CRS development via an immunogenic response to the viral proteins.[17]

Lastly, the use of viral vectors for gene therapy brings the risk of mutagenesis. Especially when using integrating vectors such as retro- and lentiviruses, the host genome can be affected by integration of the transgene.[18] While gene integration is often biologically silent, or biologically and clinically irrelevant, the transgene can also be inserted into proto-oncogenes and cause gain-of-function mutations that activate the gene.[18] Although this risk is smaller in *ex-vivo* transduction due to the possibility of pre-screening the transduced cells, the occurrence of such an event can have catastrophic consequences, as demonstrated by early trials with retroviral gene therapy for boys with a form of immunodeficiency (SCID-X1). Their disease was successfully treated, but 4 of the 9 boys later developed T-cell leukaemia due to insertion into proto-oncogenes.[19]

Besides the risks and side-effects associated with viral vectors, the manufacturing process also has several limitations. Firstly, the production process of viruses is long and complex,[20] adding to the total time of the production process, which is around 22 days.[21] As the patients often suffer from advanced tumours, this delay in treatment can lead to tumour progression and decreased life expectancy. Secondly, viral vectors are limited in the amount of cargo they can carry, which can limit the targets and types of CAR receptor used.[22] Lastly, the production of viral vectors is very costly, contributing to the high therapy costs of CAR T-cell therapy.[20] The current price of a single CAR T-cell infusion lies between $373 000 and $475 000.[23] This estimation does not include the costs for hospital stay and additional treatments, which can add another $300 000 to $500 000.[23] This high cost is a big barrier to wide-spread implementation, as demonstrated by the fact that a total of only 20.000 patients have been treated with CAR T-cell therapy world-wide in the 6 years it has been commercially available.[24] The cost-effectiveness of CAR T-cells is considered largely acceptable due to the great health benefits gained. However, budget impact analysis showed that less than half of the eligible patients could be treated at current pricing before budget impact thresholds are crossed, a threshold indicating when the costs are too high for the health care system to absorb.[23]

To address all of these drawbacks, alternative non-viral CAR T-cell engineering methods could be used. One option for this is the use of mRNA, which offers many advantages over viral vectors. First, the safety profile of mRNA is far superior, as it stays in the cytoplasm of the cell and is not integrated into the genome, preventing insertional mutagenesis. Moreover, the transient expression reduces the risk for B-cell aplasia.[20,25] Secondly, the level of protein production from the mRNA can be tightly controlled by

modifying the mRNA to increase or decrease stability of the molecule.[26] Lastly, large scale production of mRNA is quite fast, simple, cheaper than the manufacturing and safety controls needed for the production of viral vectors, and can be done under standardised and controlled conditions.[25] Nevertheless, mRNA also has its limitations. Naked mRNA degrades very quickly and is unable to cross the cell membrane. Therefore, a vector or delivery method is needed to deliver the mRNA to the cytosol.

Currently, electroporation is the most used delivery method for nucleic acids, a physical transfection method in which short high voltage pulses are applied to transiently disrupt the cell membrane and allow for the RNA to enter by passive diffusion. Several studies have been performed using electroporated RNA-based CAR T-cells, *in vitro*, in animal models, and even in human trials.[27-36] In a variety of cancers, including ALL and Hodgkin's lymphoma, mRNA-based CAR T-cell therapy was shown to cause cancer cell lysis and a decrease in tumour burden.[27-36] On short term, the efficacy of mRNA-based CAR T-cell therapies was similar to viral-based CAR T-cell therapies.[27,28,33] Additionally, it was shown that the expression level of the CAR construct can be regulated by modulating the amount of RNA delivered to the T-cells, while the percentage of CAR-positive cells remains the same.[27] This resulted in an RNA dose-dependent decrease in cytokine secretion (IL-2 and IFN-γ), which can potentially help in controlling side-effects such as CRS.[27]

These trials show the great potential of RNA-based CAR T-cell therapy. However, the use of electroporation as a delivery method can limit the true potential, since electroporation can lead to high cytotoxicity and unreliable transfection rates.[20] Additionally, it has been shown to affect T-cell activation. Electroporation leads to immediate non-specific activation of the T-cells with high increases in cytokine secretion, followed by a period of diminished antigen-specific effector function, which can affect CAR T-cell function.[37] An alternative is chemical transfection, via the use of nanoparticles composed of either lipids or polymers. In particular lipid nanoparticles (LNPs) have shown significant potential for RNA delivery, as demonstrated by the FDA and EMA approval of the first siRNA LNP formulation, Onpattro, for the treatment of hereditary transthyretin amyloidosis.[38] Billingsley *et al.* showed a successful CAR T-cell generation using various LNP formulations.[20,39] These reached similar transfection rates to electroporation, with a substantial decrease in cytotoxicity. Additionally, cancer killing rates of the T-cells were similar for the LNP formulations, electroporation, and viral transfection.[20,39] Although this shows great promise for RNA-based CAR T-cell therapy using LNPs, T-cells are considered "hard-to-transfect" cells due to their resistance to transfection with commonly used chemical transfection agents such as Lipofectamine®2000 or PolyFect™.[40] Therefore, extensive tests and optimalisation is needed to achieve optimal benefit of mRNA delivery to T-cells by LNPs.

In general, LNPs consist of four components; ionizable cationic lipids, amphipathic phospholipids, cholesterol, and poly ethylene glycol (PEG) lipids, which all have specific functions that help in the delivery of the cargo.[39] The ionizable lipid switches from neutral to positive in an acidic environment, which mediates two important functions. First, it allows for easy RNA encapsulation as the positive charge leads to complexation with the negatively charged RNA molecules. Second, it plays an important role in endosomal escape, as the lipids gain a positive charge in the acidic endosome and bind to the negatively charged lipids of the endosomal membrane.[41] This induces the formation of non-bilayer hexagonal structures, which lead to membrane fusion and consequent escape of the RNA.[41] The phospholipids provide structural support and also promote endosomal escape due to their fusogenic properties. The cholesterol stabilises the LNP, and the PEG prevents both clearance from the bloodstream when the LNPs are used *in vivo* and aggregation of the LNPs.[39] To reach higher transfection, a targeting agent can be added to the LNPs to increase transfection via receptor-mediated endocytosis.

Previous experiments in our lab revealed CD44, an adhesion receptor involved in cell migration, is expressed on both unstimulated and stimulated T-cells (*Fig. 1*). Although the amount of receptor per cell increases after stimulation, as shown by the mean fluorescence intensity (MFI), all cells are positive for CD44 expression even before stimulation. This marks CD44 as a potential target for receptor-mediated endocytosis on T-cells, which can be accomplished by adding a CD44-binding ligand to LNP formulations. The main ligand for CD44 is a hyaluronic acid (HA), a linear polysaccharide consisting of N-acetylglucosamine and glucuronic acid units.[42] It is a critical component of the extracellular matrix, contributing to its structural integrity and development.[43] Additionally, has a function in many different areas of the human body, such as response to tissue injury, inflammation, cell migration, and cancer formation. Interestingly, HA can have various, sometimes contrasting effects, such as either pro- or anti-inflammatory actions. The action of HA depends on several variables, including the size of HA, chemical modifications, crosslinking patterns, HA synthesis and degradation, and receptor engagement and downstream signalling.[43] HA is able to interact with several receptors and molecules, among which CD44, RHAMM, TSG6, GHAP, ICAM-1, and LYVE-1. Of these, CD44 is considered the primary HA receptor.[44]

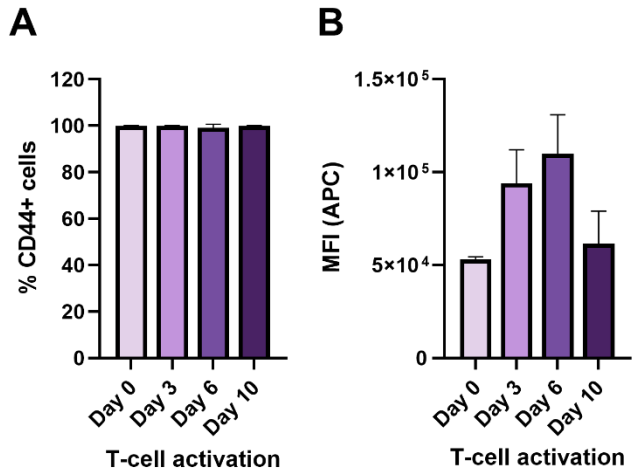


***Figure 1.*** *CD44 expression on unstimulated and stimulated T-cells.* ***A)*** *Percentage of CD44-positive T-cells before and after stimulation.* ***B)*** *Mean Fluorescent Intensity (MFI) of CD44-positive T-cells before and after stimulation.*

The addition of HA to LNP formulations has several advantages. First, transfection could be increased due to the interaction of HA with CD44.[45] Although CD44 is expressed on many cell types, this does not guarantee HA binding, as the binding of HA to CD44 is dependent on the activation state of the receptor.[46] The activation state of CD44 is regulated by post-translational modifications, in particular N-glycosylation. It was shown that cells with activated CD44 had little to no N-glycosylation on the CD44 receptor. Additionally, cells with inactivated or low-binding CD44 were converted to a more active state by the inhibition of N-glycosylation.[46] Whereas resting T-cells tend to be incapable of binding to HA, CD44-HA binding on T-cells can be activated by T-cell receptor/CD3 stimulation and inflammatory cytokines and chemokines, both in vitro and during an in vivo allogeneic response.[47-50] In addition to CD44, TSG-6, another molecule interacting with HA, is upregulated in inflammation-activated peripheral blood mononuclear cells (PBMCs), which includes T-cells.[51] TSG-6 promotes cross-linking of HA and consequently increases CD44-HA binding.[51] Second, HA has many moieties that allow for easy modification, which can facilitate for example conjugation to lipids in the LNP formulation.[45] Alternatively, electrostatic HA coating can also easily be used on cationic LNPs due to anionic charge of HA. Third, the anionic charge of HA can create a shielding effect which prevents both interaction with serum proteins and reduces cytotoxicity of cationic formulations, as cationic charges are known to

increase cytotoxicity due to plasma membrane disruption and mitochondrial and lysosomal damage.[45,52] And last, the presence of HA in the formulation allows for lyophilisation, which can increase the stability and shelf life of the product.[45] This facilitates the manufacturing process as LNPs can stored for longer instead of formulated on demand, which can reduces the costs of therapy.

Although the addition of HA to LNPs has never been tested for the delivery to T-cells, it has been used in various other contexts. CD44 is a receptor that is expressed constitutively throughout the body, as well as expressed in high levels on cancer cells. Due to this, HA has been tested to increase cargo delivery of nanoparticles in the context of tumour therapy, ocular gene therapy, and delivery to macrophages and monocytes.[53-63] In cancer, it was shown that the addition of HA to the nanoparticles selectively increased the delivery to CD44-expressing cancer cells compared to uncoated nanoparticle formulations.[58-63] Additionally, particles with HA were shown not to exhibit high cytotoxicity, in some cases none at all, and even decrease the toxicity of the formulations that caused high cytotoxicity when uncoated.[58-61,63] In macrophages, and both retinal and corneal epithelial cells it was shown as well that HA-coating improved nanoparticle delivery of various cargoes,[53,54,57] confirming the hypothesis that HA coating can increase delivery to CD44-positive cells. In this study, we will optimise mRNA delivery to primary T-cells via HA coating of LNPs with the final goal of mRNA based CAR T-cell generation.

# 2 Materials and methods

## 2.1 T-cell isolation and culture

Primary T-cells were isolated from healthy donor buffy coats, which were obtained from the Red Cross Flanders Biobank (*Ghent, Belgium*). Buffy coats were handled according to the Medical Ethical Committee of Ghent University Hospital guidelines. PBMCs were isolated via density gradient centrifugation with Lymphoprep (*Stemcell Technologies, Vancouver, Canada*). T-cells were selected from the PBMCs via magnetic negative selection with the EasySep Human T-cell Enrichment Kit (*Stemcell Technologies, Vancouver, Canada*) according to the provided protocol. Next, isolated T-cells were activated with ImmunoCult Human CD3/CD28 T-cell activator (*Stemcell Technologies, Vancouver, Canada*) according to manufacturer's protocol and cultured for 3-6 days in Iscove's modified Dulbecco's Medium (IMDM) GlutaMAX (*Gibco, Merelbeke, Belgium*), supplemented with 10% Fetal Bovine Serum (FBS, *Biowest*), 100 U/mL penicillin and 100 µg/mL streptomycin (P/S, *Gibco, Merelbeke, Belgium*), and 10 ng/mL human recombinant IL-2 (CHO expressed) (*Stemcell Technologies, Vancouver, Canada*), at 37 °C in a 5% $CO_2$ atmosphere.

## 2.2 LNP formulation and coating

Lipid nanoparticles were generated by the vortex mixing method. The C12-200 lipid was obtained from Corden Pharma (*Plankstadt, Germany*), while all other lipids were obtained from Avanti Polar Lipids (*Alabaster, USA*). In brief, the lipids and mRNA were dissolved in ethanol and sodium acetate buffer (50 mM, pH 4), respectively, and combined while vortexing for optimal particle formation. For the removal of ethanol, the LNPs were dialysed against PBS for 1.5 hours in Pur-A-Lyzer Mini Dialysis Kit, cut-off weight 12000 (*Merck, Darmstadt, Germany*), then left overnight at 4 °C to stabilise. The ratio of chargeable polymer amine groups to negatively charged nucleic acid phosphate groups, or the N/P ratio, was set to 6 for all LNP formulations. The final composition of the DOTAP and C12-200 LNPs used is shown in *table 2*.

***Table 2.*** *Molecular composition of the formulated LNPs. % mol = molar percentage.*

| Lipid | DOTAP LNP % mol | DOTAP 0.8% LNP % mol | DOTAP 0.4% LNP % mol | C12-200 LNP % mol |
|---|---|---|---|---|
| **DOTAP** | 50 | 50 | 50 | - |
| **DOPE** | 8 | 8.5 | 8.9 | 10 |
| **Cholesterol** | 23.3 | 23.3 | 23.3 | 38.5 |
| **C12-200** | 17.5 | 17.5 | 17.5 | 50 |
| **DMG-PEG** | 1.3 | 0.8 | 0.4 | 1.5 |
| **DiD** | 0.5 | 0.5 | 0.5 | 0.5 |

For the preparation of electrostatically coated HA-LNPs or PSS-LNPs, 20 kDa HA (*BOC-sciences, Shirley, USA*) or 70 kDa PSS (*Sigma-Aldrich, Saint-Louis, USA*) was dissolved in nuclease free water (*Invitrogen, Waltham, USA*) and added to the uncoated LNPs with the volumes in an aqueous solution/LNP ratio of 2/1. The mixture was vortexed for 10 seconds and left to stabilise for 15 minutes at room temperature. The concentration of HA/PSS was expressed as a percentage of the total amount of DOTAP (DOTAP LNPs) or C12-200 (C12-200 LNPs) moles in the used formulation. For conjugated HA-LNPs, an in-house produced HA-DOPE conjugate was used. LNPs were formulated as described above and coated with HA-DOPE dissolved in nuclease free water in the same method as the electrostatic coating.

## 2.3 Characterisation of LNPs

The hydrodynamic diameter (intensity-weighted Z-average), polydispersity index (PDI), and surface charge (zeta potential) of the LNPs were analysed on the NanoZS Zetasizer (*Malvern Panalytical, Londen United Kingdom*). Z-average and PDI were measured via dynamic light scattering (DLS), and zeta

potential was calculated from the electrophoretic mobility of the LNPs. All samples were measured diluted in HEPES buffer (20 mM, pH 7.4) in triplicate. Concentration of encapsulated mRNA and encapsulation efficiency were determined using the Quant-iT RiboGreen RNA assay (*Thermofisher Scientific, Waltham, USA*). In brief, the encapsulated RNA concentration was determined by mRNA quantification in the absence and presence of Triton-X100, which allows for quantification of free and total mRNA, respectively. The encapsulated mRNA concentration was calculated by the equation:

$$Conc.(encapsulated\ mRNA) = Conc.(total\ mRNA) - Conc.(free\ mRNA)$$

The encapsulation efficiency was calculated by the equation:

$$Encapsulation\ efficiency\ (\%) = \frac{Conc.\ encapsulated\ mRNA}{Conc.\ total\ mRNA} * 100\%$$

For validation of RNA encapsulation, LNPs and RNA were separated on 1x TBE 1% agarose gel with GelRed (*Biotium, Fremont, USA*). Samples were diluted in Gel Loading Buffer II (*Invitrogen, Waltham, USA*)) and 100 ng RNA was loaded. Electrophoresis was carried out for 40 minutes at 100 V. RNA bands were visualised using UV lighting.

## 2.4 T-cell transfection with LNPs

LNP transfection was performed on activated and expanded T-cells, on day 3 and 6 after stimulation. Transfection was performed in ImmunoCult™-XF T-cell Expansion Medium (*Stemcell technologies, Vancouver, Canada*). The cells were seeded into a 96-well plate at a density of 50.000 cells/well and cultured with the LNPs at a concentration of 1 ng/µL mRNA in 100 µL. For transfections in Opti-MEM™ (*Gibco, Merelbeke, Belgium*), cells were cultured with LNPs in Opti-MEM for 1 and 4 hours, then spun down and resuspended in Immunocult™-XF medium. Read-out of the transfection was performed 24 hours after addition of the LNPs. eGFP expression and LNP uptake were quantified via flow cytometry on a cytoFLEX Flow Cytometer (*Beckman Coulter, Indianapolis, USA*). Flow cytometry data was analysed using FlowJo v10.7.2 software (*BD Biosciences, Franklin Lakes, USA*). Cell viability was evaluated with the CellTiter-Glo Luminescent Cell Viability Assay (*Promega, Leiden, the Netherlands*). In brief, the cells were supplemented with an equal volume of CellTiter-Glo reagent, and mixed for 10 minutes on an orbital shaker at 120 rounds per minute. Cell lysate was transferred to an opaque 96-well plate and luminescence was measured on a GloMax Navigator Microplate Reader (*Promega, Leiden, the Netherlands*). Cell viability was calculated relative to the non-treated control. The delivery yield, a parameter showing the percentage of viable and successfully transfected cells, was calculated with the following equation:

$$Yield\ (\%) = \frac{Cell\ viability\ (\%) * Transfected\ cells\ (\%)}{100}$$

## 2.5 HA-FITC titration with CD44 blocking

HA-FITC titration to test for HA binding on T-cells was performed on day 3 and 6 after T-cell activation. The cells were seeded into a 96-well plate at a density of 100.000 cells/well, and incubated in Human TruStain FcX™ FC-blocking solution (*Biolegend, San Diego, USA*) for 20 minutes at room temperature. Subsequently, the cells were incubated with 2 µg/mL APC anti-human CD44 (*Biolegend, San Diego, USA*) for 30 minutes at 4 °C. Next, the cells were resuspended in various concentrations of 50 kDa HA-FITC (*Haworks, Bedminster, USA*) in Immunocult™-XF medium and incubated for 2 hours at 37 °C. HA-FITC and anti-CD44 binding was analysed on a cytoFLEX Flow Cytometer (*Beckman Coulter, Indianapolis, USA*). Flow cytometry data was analysed using FlowJo v10.7.2 software (*BD Biosciences, Franklin Lakes, USA*).

## 2.6 Fluorescent Correlation Spectroscopy (FCS)

The stability of HA-coating on the LNPs in medium was determined with fluorescent correlation spectroscopy (FCS). FCS is a fluorescent microscopy based technique, in which the continuous movement of fluorescent molecules in and out of the detection volume is measured. Fully characterised LNPs coated with Cy-5 labelled HA were incubated for 4 hours at 37 °C in ImmunoCult™-XF and Opti-MEM in a concentration equivalent to the used concentration for transfection. Control conditions were incubated in HEPES (20 mM, pH 7.4) for 4 hours at 4 °C. After incubation, samples were diluted to 10 µg/mL HA-Cy5 in 50 µL in a glass-bottom 96-well plate (*Greiner, Kremsmünster, Austria*). Fluorescent time traces were obtained through excitation of a small volume with a 640 nm laser through a water immersive lens (60x Plan Apo VC, N.A. 1.2, Nikon) on a confocal microscope (Nikon A1R) at approximately 50 µm above the bottom of the glass plate. Fluorescent signal was recorded by a photon counting instrument (PicoHarp, 300, PicoQuant) in timeframes of 60 seconds.

## 2.7 Statistical analysis

Data analysis was done using Graphpad Prism 8 software. All data is presented as mean ± standard deviation (SD). Unless stated otherwise, data consists of technical replicates rather than biological replicates. When biological replicates were available, statistical significance was tested with a one-way ANOVA. Homoskedasticity and normality of the residuals were determined with a Brown-Forsythe test and QQ-plot, respectively. Multiple T-tests with Tukey's correction was used for comparing all groups.

# 3 Results

## 3.1 Electrostatic HA coating decreases transfection of cationic DOTAP LNPs in primary T-cells

To enable electrostatic coating, a cationic LNP formulation previously described in literature was chosen.[64] The DOTAP formulation contains the standard components of LNP formulations, but is supplemented with 50% of the permanently cationic 1,2-dioleoyl-3-trimethylammonium-propane (DOTAP) lipid. This results in an LNP with a strong cationic charge that can interact with anionic molecules. For the electrostatic coating, HA was added to the formulated LNPs in various concentrations and vortexed to ensure proper mixing. After a short incubation to allow the HA-LNP complexes to stabilise, the coating was characterized with dynamic light scattering (DLS). First, a concentration range of HA was tested on empty LNP formulations to determine the optimal coating concentration (*Tab. 3*). Uncoated, the DOTAP formulation has a size of around 150 nm, with a PDI of around 0.3, which means the formulation is largely stable, but prone to forming a small amount of aggregates. The charge of uncoated empty DOTAP LNPs lays around +20 mV. After HA coating, size and PDI remain mostly stable, with some size fluctuations between 100-200 nm. However, as this variation is seen between different uncoated LNP batches as well, these fluctuations are not likely to be caused by the coating. The charge of the LNPs drops dose-dependently with the addition of HA, indicating a HA-LNP complex is formed. The lowest charge measured was -24.7 mV, which we considered to be the lowest charge achievable with HA coating based on previous experience with HA-LNPs. For future experiments with HA-LNPs, the coating concentrations of 5% and 25% HA were chosen to proceed.

***Table 3.*** *Size, PDI and charge of empty DOTAP formulations with various HA coating concentrations. Concentration of HA is expressed as molar percentage of the total amount of DOTAP moles. n=3.*

| LNP | Size (nm) | PDI | Zeta potential (mV) |
|---|---|---|---|
| **Control** | 146,5 ± 8,97 | 0,293 ± 0,02 | 22,5 ± 1,39 |
| **0.25% HA** | 196,9 ± 0,80 | 0,379 ± 0,01 | 12,6 ± 1,31 |
| **0.5% HA** | 163,0 ± 9,98 | 0,380 ± 0,06 | 0,9 ± 0,54 |
| **1% HA** | 167,5 ± 4,96 | 0,442 ± 0,08 | -10,7 ± 0,83 |
| **2% HA** | 151,8 ± 6,11 | 0,379 ± 0,07 | -12,9 ± 0,61 |
| **10% HA** | 151,1 ± 1,81 | 0,391 ± 0,02 | -14,4 ± 1,07 |
| **25% HA** | 151,2 ± 6,77 | 0,398 ± 0,01 | -16,8 ± 2,03 |
| **50% HA** | 114,4 ± 4,13 | 0,282 ± 0,03 | -18,5 ± 0,49 |
| **100% HA** | 112,9 ± 2,54 | 0,246 ± 0,01 | -22,7 ± 0,30 |
| **200% HA** | 124,5 ± 9,53 | 0,359 ± 0,03 | -24,7 ± 2,43 |

Next, DOTAP LNPs containing enhanced green fluorescent protein (eGFP) and luciferase mRNA were formulated, coated, and characterised (*Tab. 4*). The addition of mRNA did not affect the size, PDI or charge of the LNPs. Additionally, both uncoated and coated LNPs have a very high mRNA encapsulation.

***Table 4.*** *Size, PDI, charge, and encapsulation efficiency of DOTAP LNPs containing eGFP and luciferase mRNA. Table represents the average of four separate LNP batches (N=4). Luc = Luciferase.*

| LNP | | Size (nm) | PDI | Zeta potential (mV) | Encapsulation efficiency (%) |
|---|---|---|---|---|---|
| **eGFP** | **Control** | 163,8 ± 24,7 | 0,265 ± 0,06 | 13,4 ± 2,44 | 98,8 ± 2,67 |
| | **5% HA** | 186,2 ± 30,6 | 0,251 ± 0,08 | -16,1 ± 4,85 | 96,0 ± 7,82 |
| | **25% HA** | 178,0 ± 33,4 | 0,246 ± 0,07 | -17,6 ± 2.43 | 95,7 ± 7,64 |
| **Luc** | **Control** | 158,0 ± 34,8 | 0,269 ± 0,05 | 13,2 ± 5,41 | 98,8 ± 2,72 |
| | **5% HA** | 168,6 ± 25,0 | 0,272 ± 0,09 | -17,1 ± 4,11 | 95,9 ± 7,70 |
| | **25% HA** | 172,7 ± 43,7 | 0,281 ± 0,06 | -18,8 ± 2,79 | 95,8 ± 7,71 |

To determine the effect of HA coating on the transfection, uptake, and cytotoxicity of the LNPs in primary T-cells, T-cells were isolated and transfected with the LNPs on day 3 post-activation. Luciferase LNPs were used as control for autofluorescence of T-cells induced by the LNP treatment. Accordingly, gates were set on the luciferase control. Uncoated eGFP DOTAP LNPs were able to transfect around 35% of the T-cells (*Fig. 2A*). However, HA coating did not increase the transfection as expected. Rather than increase, both the percentage of eGFP-positive cells and the fold-MFI (fMFI) of the transfected

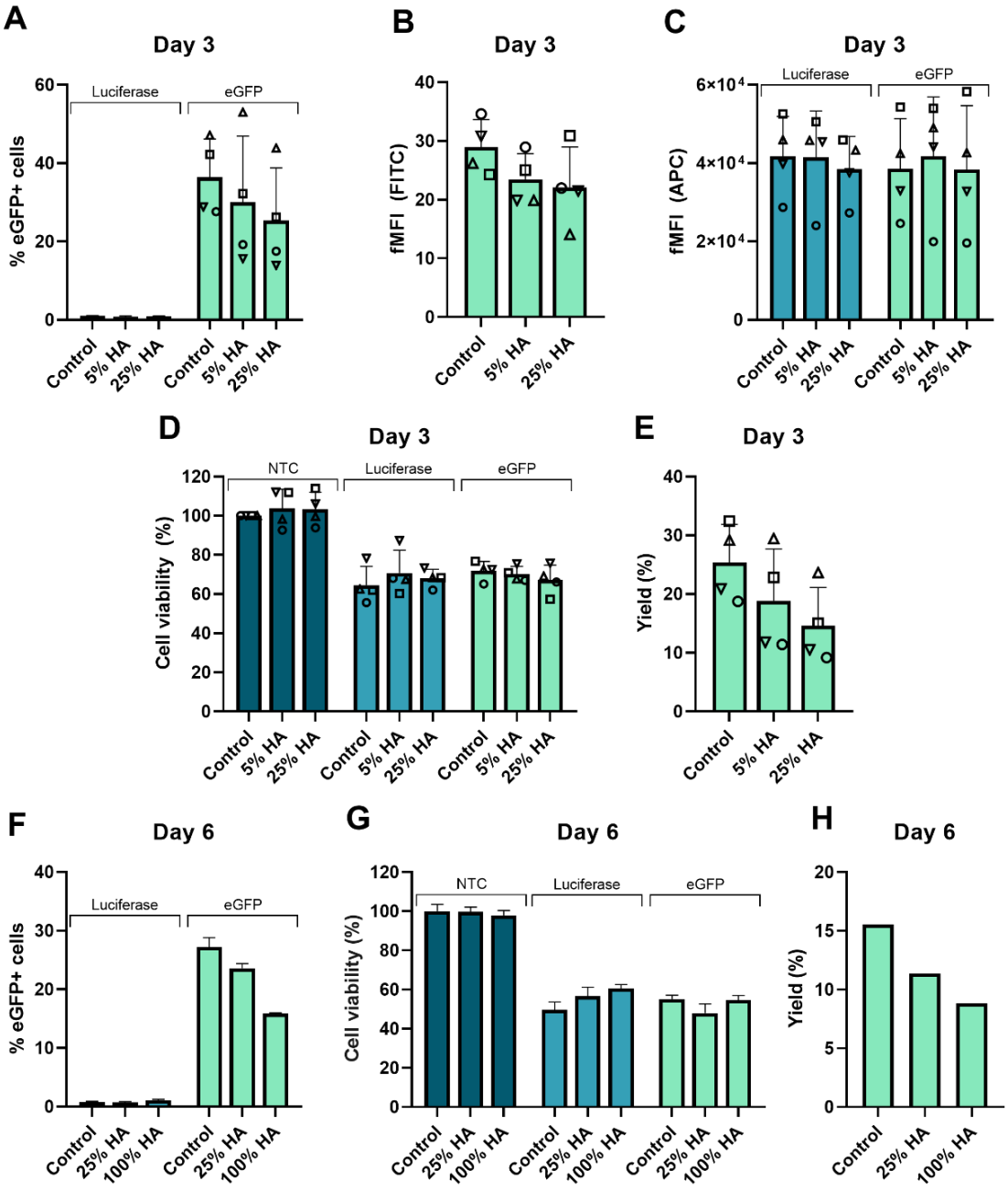


***Figure 2.*** *Analysis of transfection efficiency and cytotoxicity of HA-coated DOTAP LNPs on primary T-cells 3 and 6 days post-activation.* ***A-B)*** *Percentage of eGFP-positive cells and fMFI of eGFP-positive cells after transfection on day 3.* ***C)*** *fMFI of LNP-positive cells on day 3.* ***D)*** *Cell viability of primary T-cells after transfection on day 3.* ***E)*** *Yield of viable transfected cells on day 3.* ***F)*** *Percentage of eGFP-positive cells after transfection on day 6.* ***G)*** *Cell viability of primary T-cells after transfection on day 6.* ***H)*** *Yield of viable transfected cells on day 6. Data of transfections on day 3 represents biological replicates (N=4). Data of transfections on day 6 represents technical replicates (n=3). NTC = Non-Treated Control.*

cells decreased (*Fig. 2A-B*). Although the decrease was not statistically significant due to large variation in transfection efficiency between the different T-cell donors, the decrease can consistently be seen for all donors. Uptake of the LNPs was analysed by detection of the lipid dye DiD on flow cytometry. HA coating did not visibly affect the uptake of the LNPs. The percentage of LNP-positive cells was 100% in all conditions (*Fig. S1A*). However, flow cytometry cannot distinguish between actual uptake and LNPs sticking to the outside of the cell. Previously performed microscopy experiments have shown that the cells measured on flow cytometry as LNP-positive are a mix of cells with internalised LNPs and cells with LNPs sticking to the cell membrane (*Fig. S1B-C*). Nevertheless, the fMFI for uptake (APC) remains the same in all conditions (*Fig. 2C*), confirming that HA coating does not affect uptake or interaction between cells and LNPs. The expected decrease in cytotoxicity after HA coating was not seen (*Fig. 2D*). Transfection with DOTAP LNPs decreased cell viability to approximately 60% relative to the untreated control, with no differences between the uncoated and coated conditions. All in all, the overall yield of viable transfected cells showed a consistent decrease with the addition of HA coating. Since it was shown previously that the CD44 expression level on T-cells can increase on day 6 compared to day 3 post-activation (*Fig. 1*), we repeated the transfection on day 6 (*Fig. 2F-H*). However, the effect of HA-coating on day 6 was equivalent to day 3. The transfection efficiency decreases, while cytotoxicity level of distinct LNP formulations are equivalent, resulting in an overall lower yield.

## 3.2 PEG percentage of LNP formulations does not influence the effect of HA coating.

To determine if the presence of PEGylated lipids might be interfering in HA-LNP interaction and affecting transfection through prevention of a stable HA coating, LNP formulations with lower percentages of DMG-PEG were formulated, coated, and characterised (*Tab. 5*). With a decreasing percentage of PEG, LNP size expanded slightly. PDI remained mostly stable but a small increase in aggregate presence could be seen in the LNP with 0.4% PEG (*Fig. S2*). However, all LNPs still gave a strong negative charge when coated with HA and a high mRNA encapsulation efficiency.

***Table 5.*** *Size, PDI, charge, and encapsulation efficiency of DOTAP LNPs with 1.3%, 0.8% and 0.4% of PEG-DMG included in the formulation.*

| LNP | | Size (nm) | PDI | Zeta potential (mV) | Encapsulation efficiency (%) |
|---|---|---|---|---|---|
| **1.3%** | **Control** | 154,1 ± 7,33 | 0,289 ± 0,02 | 17,2 ± 3,85 | 99,3 ± 0,06 |
| | **5% HA** | 180,9 ± 9,20 | 0,296 ± 0,04 | -16,7 ± 1,91 | 97,5 ± 0,40 |
| | **25% HA** | 159,7 ± 10,50 | 0,252 ± 0,04 | -19,4 ± 2,45 | 97,6 ± 0,52 |
| **0.8%** | **Control** | 175,5 ± 24,76 | 0,288 ± 0,04 | 24,6 ± 9,58 | 99,1 ± 0,21 |
| | **5% HA** | 224,4 ± 33,64 | 0,252 ± 0,03 | -18,6 ± 3,00 | 97,0 ± 0,40 |
| | **25% HA** | 195,6 ± 36,38 | 0,229 ± 0,03 | -19,9 ± 3,21 | 96,7 ± 0,18 |
| **0.4%** | **Control** | 204,2 ± 53,40 | 0,298 ± 0,04 | 34,2 ± 5,03 | 99,1 ± 0,27 |
| | **5% HA** | 368,4 ± 93,21 | 0,324 ± 0,07 | -21,8 ± 1,45 | 97,5 ± 0,52 |
| | **25% HA** | 302,3 ± 24,19 | 0,260 ± 0,06 | -24,3 ± 1,38 | 97,0 ± 0,72 |

In the transfection, no big differences could be seen in the effect of HA coating between the different formulations. In the formulations with 0.8 and 0.4% of PEG-DMG, the transfection efficiency of the uncoated particles decreased compared to the control formulation with 1.3% PEG-DMG (*Fig. 3A*). This might be due to the formation of aggregates induced by lower PEG presence. Due to the decrease in transfection efficiency for the uncoated particles, the differences between the uncoated and coated conditions are smaller, but still a clear decrease in transfection can be observed in the HA-coated conditions. The HA-coated luciferase control LNPs with 0.8% PEG-DMG gave a surprisingly high percentage of eGFP-positive cells, indicating strong autofluorescence. This is probably due to pipetting

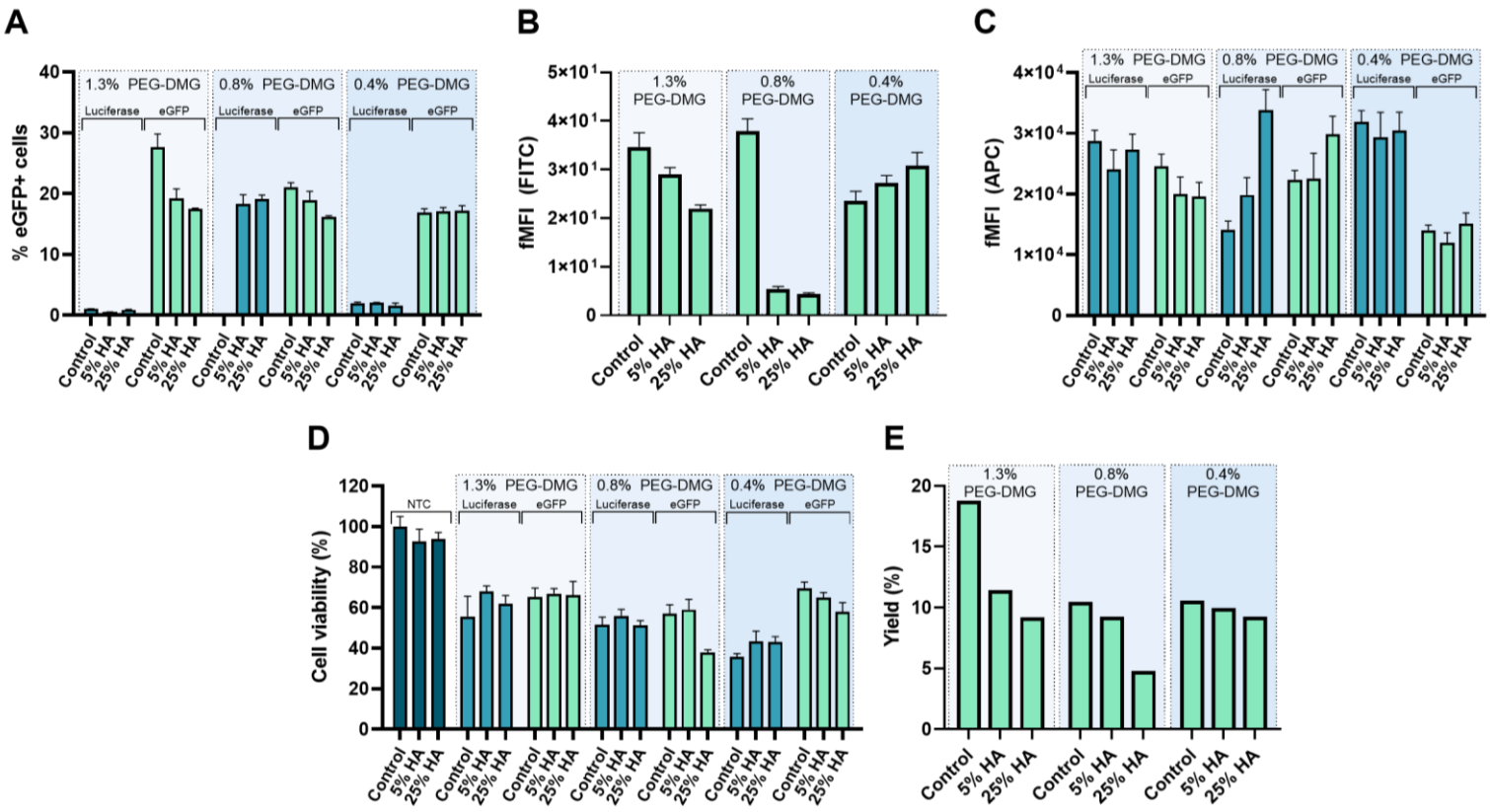


***Figure 3.*** *Analysis of transfection efficiency and cytotoxicity of HA-coated DOTAP LNPs with various PEG-DMG concentrations.* ***A-B)*** *Percentage of eGFP-positive cells and fMFI of eGFP-positive cells after transfection.* ***C)*** *fMFI of LNP-positive cells.* ***D)*** *Cell viability of primary T-cells after transfection.* ***E)*** *Yield of viable transfected cells. NTC = Non-Treated Control.*

error or mix-up of certain conditions. Accordingly, regarding the fMFI of the transfected cells, no conclusions can be drawn from the big decrease in fMFI of the HA-coated 0.8% LNPs (*Fig. 3B*). Therefore, these data will not be taken in to account for further analysis. The fMFI of the 0.4% LNPs shows a small increase in the HA-coated conditions. However, as the increase is very small and not seen in any other conditions or transfections, it is more likely to be a coincidental difference or pipetting error than HA-dependent increase. Uptake fMFI is variable, but no clear patterns or consistent relevant differences between conditions could be seen (*Fig. 3C*). Some of the variation in uptake fMFI might be due to differences in the number of LNPs added. As LNP dilution for transfection is based on encapsulated mRNA concentration, LNP formulations with a lower encapsulated mRNA concentration are diluted less, and thus could contain more LNPs. Cell viability is comparable between the different formulations, although the LNPs with lower PEG content might be slightly more cytotoxic (*Fig. 3D*), which might be caused by the presence of some LNP aggregates in these formulations. Overall, yield of the uncoated LNPs decreases strongly with lower PEG presence, and HA coating decreases the yield further in all LNP formulations (*Fig.3E*). The amount of PEG in a formulation does not clearly influence the effect of HA coating and is thus unlikely to be interfering in HA-LNP interactions. Considering stability of the LNPs with lower PEG concentration was decreased as well, work with these formulations was discontinued.

## 3.3 HA binds to primary T-cells both specifically and aspecifically

As described earlier, expression of CD44 does not guarantee HA-binding. Specifically, activation state of the CD44 receptor determines the ability of CD44 to bind to HA. According to literature, T-cell activation should induce HA-binding state of CD44 on T-cells. To confirm this and to determine whether an inability of the receptor to bind HA is responsible for the lack of increased transfection of HA-LNPs,

a titration of fluorescently labelled HA on T-cells was performed on day 3 and day 6 post-activation. Additionally, anti-CD44 antibodies were used to block the CD44 receptor to confirm specific binding of HA to CD44. The percentage of HA-binding cells increased dose-dependently of HA, while the amount HA molecules binding per cell, represented by the fMFI, remained equal regardless the dose of HA (*Fig. 4A-B*). Interestingly, the overall fMFI of day 6 was much lower than on day 3, which can be explained by a shift in the overall cell population on day 6. Whereas both activated and inactive populations of T-cells can be seen on day 3, defined respectively as forward scatter(FSC)-high and FSC-low cells, all T-cells shift to the activated population on day 6 (*Fig. S3A-B*). In this activated population, the HA-positive cells have little lower MFI, while the overall population has a slightly higher MFI. Since the fMFI is the ratio of MFI of the positive population over the MFI of the overall population, this leads to a low fMFI compared to day 3. All T-cells expressed CD44 on both days as was shown previously (*Fig. 4C*). The fMFI of CD44-positive cells is lower on day 6 (*Fig. 4D)*, which can again be explained by the shift in population (*Fig. S3C-D*). Blocking the Fc-receptor with Fc-block did not affect HA-binding on day 3, while HA-binding was slightly lower in the presence of CD44 (*Fig. 4E-F*). On day 6, Fc-block had a larger effect and led to a small but clear decrease in HA-binding, indicating some HA might be binding to the Fc receptor on day 6. Fc-receptor expression on T-cells is known vary depending on the activation cycle of T-cells,[65] which explains why HA seems to bind to the Fc-receptor on day 6, but not on day 3. On day 6, anti-CD44 had a much less clear effect on HA binding. Overall, anti-CD44 antibodies might be able to prevent cell and binding to alternative proteins such as the Fc-receptor, or the used anti-CD44 antibody does some HA binding, but does not completely block it. Either part of the HA is sticking aspecifically to the

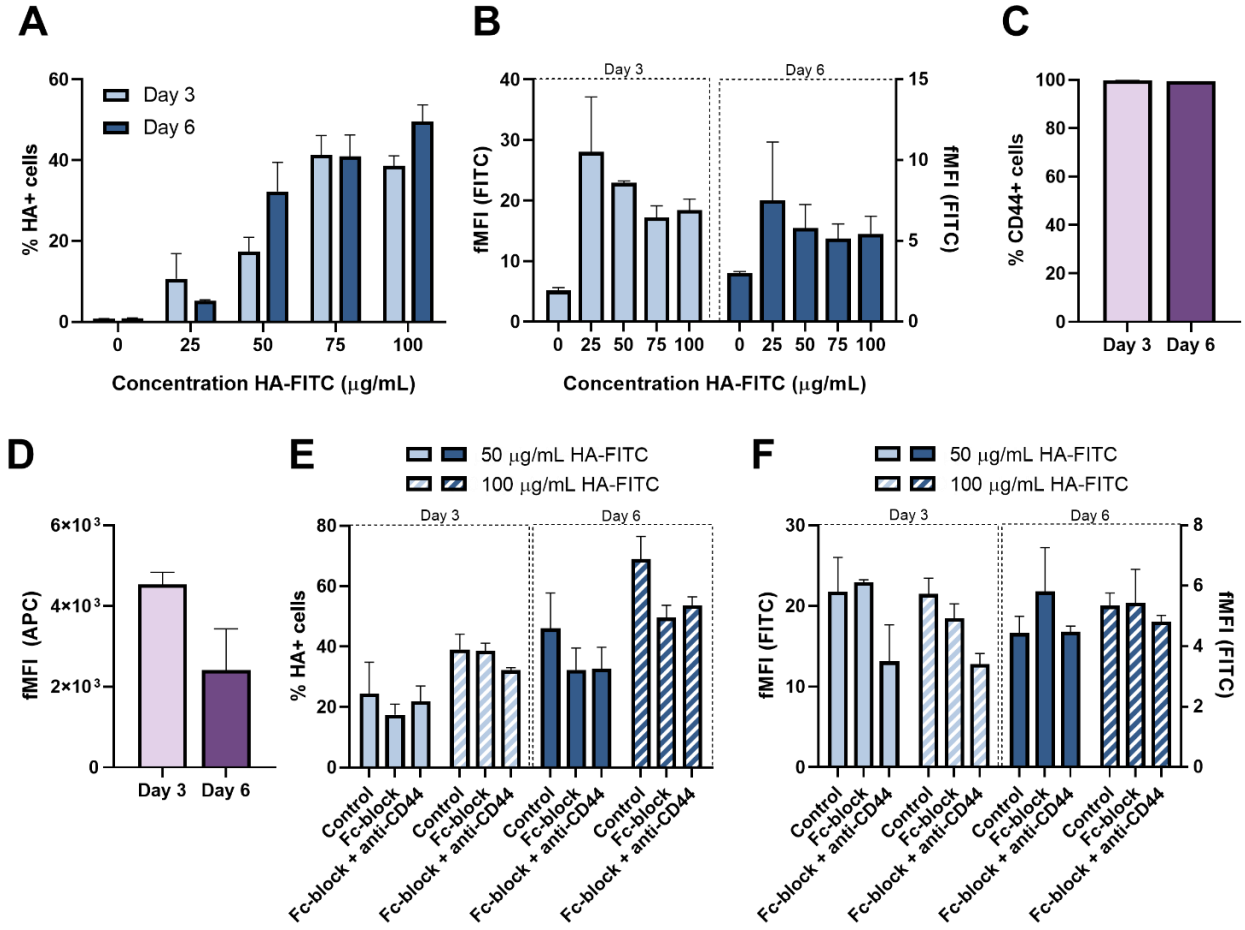


***Figure 4.*** *Flow cytometry analysis of HA-FITC titration on activated primary T-cells on day 3 and day 6 post-activation.* ***A-B)*** *Percentage and fMFI of HA-positive T-cells after incubation with various concentrations of HA-FITC.* ***C.*** *Percentage of CD44-positive T-cells.* ***D)*** *fMFI of CD44-positve T-cells.* ***E-F)*** *Percentage and fMFI of HA-positive T-cells in the presence of FC-block and anti-CD44 antibody.*

not fully block the binding epitope of HA on CD44. Altogether, it can be concluded that there is strong binding of HA to the T-cells, but it is unclear whether this binding is specific to the CD44 receptor.

## 3.4 Conjugate HA-DOPE coating has equivalent effect to electrostatic HA coating

Even though we were unable to show the binding of HA to CD44 specifically, the HA titration showed there is strong binding of HA to the primary T-cells, indicating that inability of HA to bind to the T-cells is not the cause of lower transfection efficiency. It has previously been proposed in literature that conjugate HA coating might give a more stronger increase in transfection efficiency than electrostatic due to a higher stability in the cell culture medium used during transfection.[57] Therefore, a conjugated HA coating was tested. HA-DOPE was dissolved in water, mixed with the formulated DOTAP LNPs, incubated for 15 minutes, and characterised (*Tab. 6*). Size and PDI of the LNPs increased slightly with 25% HA-DOPE coating. Charge of the LNPs was similar to electrostatically coated LNPs, suggesting that a comparable HA-LNP complex was formed.

***Table 6.*** *Size, PDI, charge, and encapsulation efficiency of DOTAP LNPs coated with 5% and 25% HA-DOPE*

| LNP | Size (nm) | PDI | Zeta potential | Encapsulation efficiency (%) |
|---|---|---|---|---|
| **Control** | 147,2 ± 16,2 | 0,234 ± 0,03 | 9,7 ± 0,78 | 97,6 ± 0,25 |
| **5% HA-DOPE** | 159,8 ± 33,5 | 0,236 ± 0,04 | -12,9 ± 1,13 | 92,4 ± 0,41 |
| **25% HA-DOPE** | 190,5 ± 9,7 | 0,335 ± 0,04 | -17,4 ± 1,80 | 91,6 ± 1,38 |

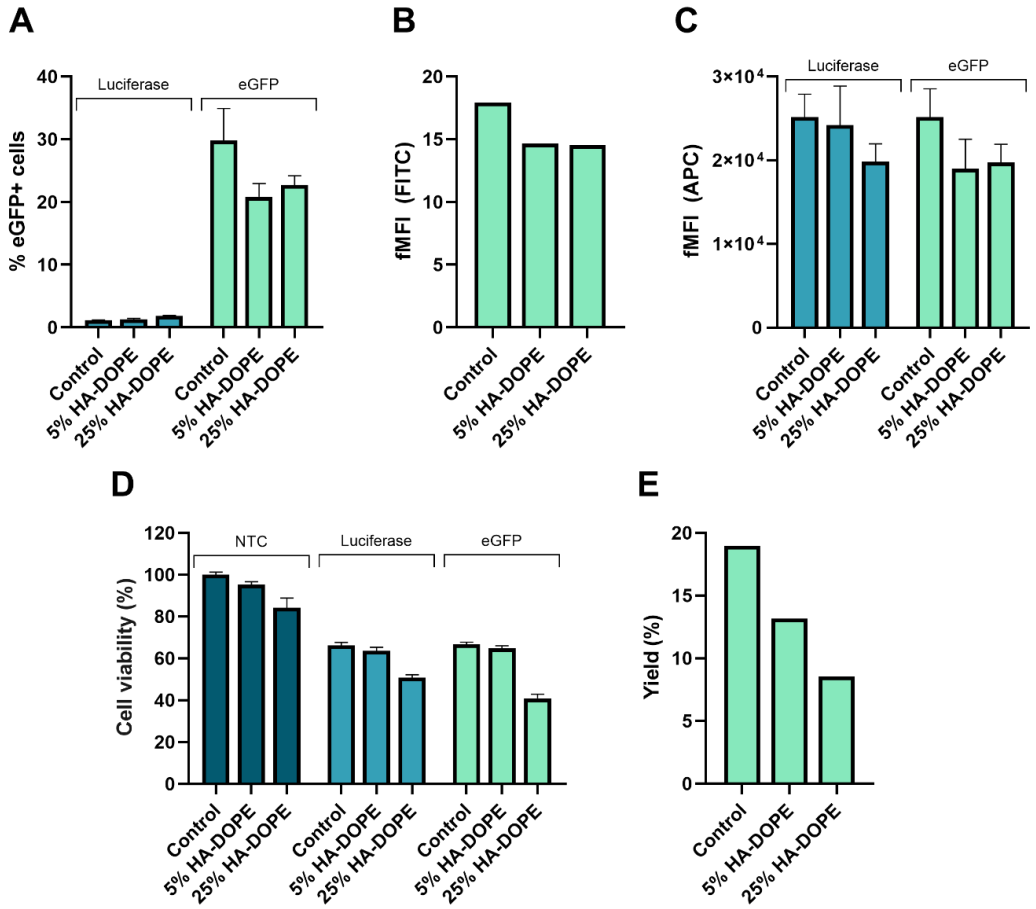


***Figure 5.*** *Analysis of transfection efficiency and cytotoxicity of DOTAP LNPs with a conjugated HA-DOPE coating.* ***A-B)*** *Percentage of eGFP-positive cells and fMFI of eGFP-positive cells after transfection.* ***C)*** *fMFI of LNP-positive cells.* ***D)*** *Cell viability of primary T-cells after transfection.* ***E)*** *Yield of viable transfected cells. NTC = Non-Treated Control. n=3.*

Regarding transfection efficiency, the results of the LNPs with conjugate HA-DOPE coating were very similar to the results of electrostatically HA-coated LNP transfections. Both the percentage and fMFI of the transfected cells decreased in the HA-coated LNP conditions (*Fig. 5A-B*). The percentage of LNP-positive cells was 100% in all conditions, which is similar to all previous transfections (*Fig. S1D*), but fMFI of uptake was also slightly decreased in the coated LNP conditions (*Fig. 5C*). Interestingly, cell viability seemed to decrease even more in the 25% HA-DOPE conditions (*Fig. 5D*). This decrease can be seen in the non-treated control with free 25% HA-DOPE as well, which suggests HA-DOPE might be a slightly cytotoxic molecule. Due to the decrease in both transfection and cell viability, an even bigger decrease in yield is seen compared to electrostatic HA coating. Nevertheless, it should be noted, the method of conjugate coating could be optimised to integrate HA-DOPE into the LNP during formulation instead of afterwards. This might yield a more stable conjugate coating, which could change the results found here.

## 3.5 More stable HA coating Opti-MEM does not provide increase in transfection efficiency

Next, an experiment to determine the stability of the HA coating in cell culture medium was set up. First, general LNP stability measurement in medium was attempted through size and PDI analysis on DLS. The LNPs were incubated in ImmunoCult™-XF for 1 hour at 37 C, and then analysed on DLS. Besides ImmunoCult™-XF, the LNPs were incubated in Opti-MEM as well, a transfection cell culture medium with minimal protein content, to see if the decreased presence of proteins could influence LNP stability. While size and PDI of the LNPs was completely stable in Opti-MEM, DLS measurement in ImmunoCult™-XF gave extreme values (*Tab. S1*). Most likely, the proteins present in the medium are influencing the measurement, leading to unreliable results. Additionally, charge, and thus stability of the HA coating, cannot be measured with DLS in in either medium, due to the ionic strength of the solutions. Therefore, a fluorescent correlation spectroscopy (FCS) experiment was performed to determine coating stability.

In FCS, a small volume is excited by a laser and the fluctuations in fluorescent signal are measured over a time frame of 60 seconds as fluorescent molecules diffuse in and out of the measured volume. A solution of free fluorescently labelled HA gives a baseline of free HA, while a solution of LNPs coated with fluorescently labelled HA should give a lower baseline of free HA and high peaks of fluorescent signal for HA-coated LNPs as multiple HA molecules on the surface of the LNP pass the detector simultaneously. The percentage of association/dissociation of HA with the LNPs can be determined by the ratio of the baseline of the free HA solution with the lower baseline of free HA in the LNP solution.

The LNPs were formulated as usual and coated with Cy5-labelled HA (50 kDA). Next, the LNPs were incubated in ImmunoCult™-XF and Opti-MEM for 4 hours at 37 °C in a dilution equal to transfection. After 4 hours of incubation, the LNPs were diluted further and fluorescent fluctuations were measured over time. The free HA solution gave a baseline of approximately 0.3 kCounts (*Fig. 6A*). In the LNP conditions, the total amount of present HA should be the same, but with a lower baseline of free HA as most of the HA is coated on the LNPs. However, in our LNP samples, the baseline of free HA is similar to the baseline of the free HA solution (*Fig. 6B-D*). Most likely, an excess of HA is present in our LNP conditions as non-bound HA is not removed after coating, which makes any difference between the conditions too small to quantify association/dissociation of HA. Nevertheless, the clear presence of HA-coated LNPs can be seen in all conditions in the form of high peaks. Coating seems to be largely stable in both ImmunoCult™-XF and Opti-MEM. However, the peaks in the ImmunoCult™-XF condition might be a little bit lower and less compared to the HEPES and Opti-MEM conditions, indicating that coating could be slightly more stable in Opti-MEM.

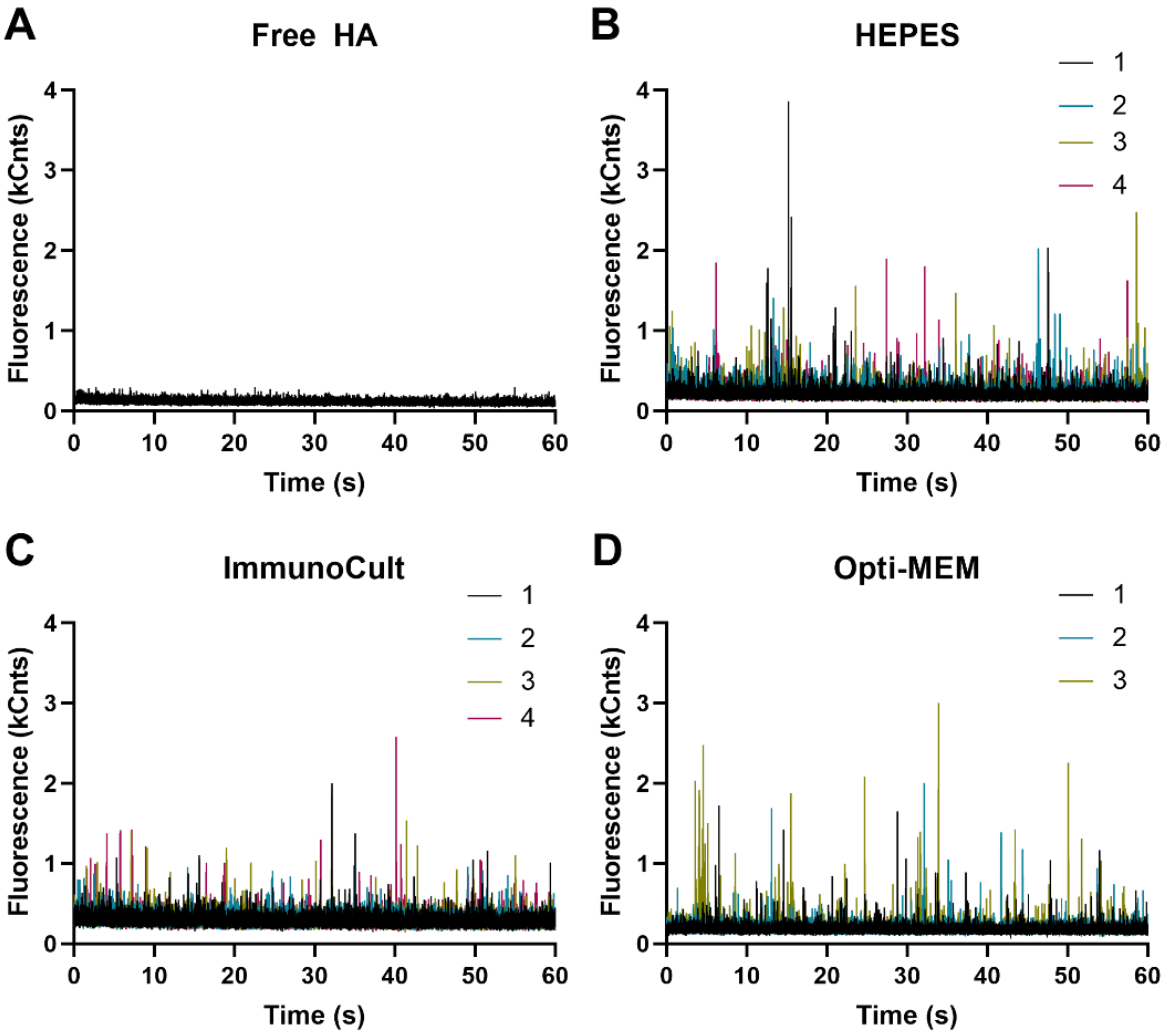


***Figure 6.*** *FCS results of DOTAP LNPs coated with HA-Cy5 in HEPES buffer, ImmunoCult™-XF, and Opti-MEM.* ***A)*** *Free HA-Cy5 in HEPES buffer.* ***B)*** *DOTAP LNPs with 5% HA-Cy5 in HEPES buffer.* ***C.*** *DOTAP LNPs with 5% HA-Cy5 in ImmunoCult™-XF after 4 hours incubation at 37 °C.* ***D.*** *DOTAP LNPs with 5% HA-Cy5 in Opti-MEM after 4 hours incubation at 37 °C. Numbers in legend represent technical replicates.*

To test if the potential better stability of our HA-coating in Opti-MEM influences the effect of HA coating, a transfection in Opti-MEM was performed. During the transfections in ImmunoCult™-XF, LNPs are added to the cells and incubated for 24 hours. Due to the minimal presence of nutrients in Opti-MEM, 24 hour incubation would cause high cytotoxicity to the T-cells. Accordingly, cells were incubated with the LNPs in Opti-MEM for 1 and 4 hours to allow LNP uptake, then transferred to ImmunoCult™-XF medium for the remaining incubation. Overall transfection increased greatly when T-cells were incubated with LNPs in Opti-MEM instead of ImmunoCult™-XF (*Fig. 7A-B*). Unfortunately, cytotoxicity strongly increased in Opti-MEM as well. Even untreated cells in Opti-MEM lose approximately 50% of cells compared to ImmunoCult™-XF, while cell transfected with LNPs in Opti-MEM lose up to 80% (*Fig. 7C*). Accordingly, the yield of transfected cells does not increase despite the higher transfection efficiency (*Fig. 7D*). Most importantly, HA coating did not improve transfection efficiency in OptiMEM compared to uncoated DOTAP. Transfection efficiency of the LNPs still decreases when coated with HA, leading to lower yield. This indicates that the proteins present in the medium are not the limiting factor for improvement of transfection efficiency mediated by HA.

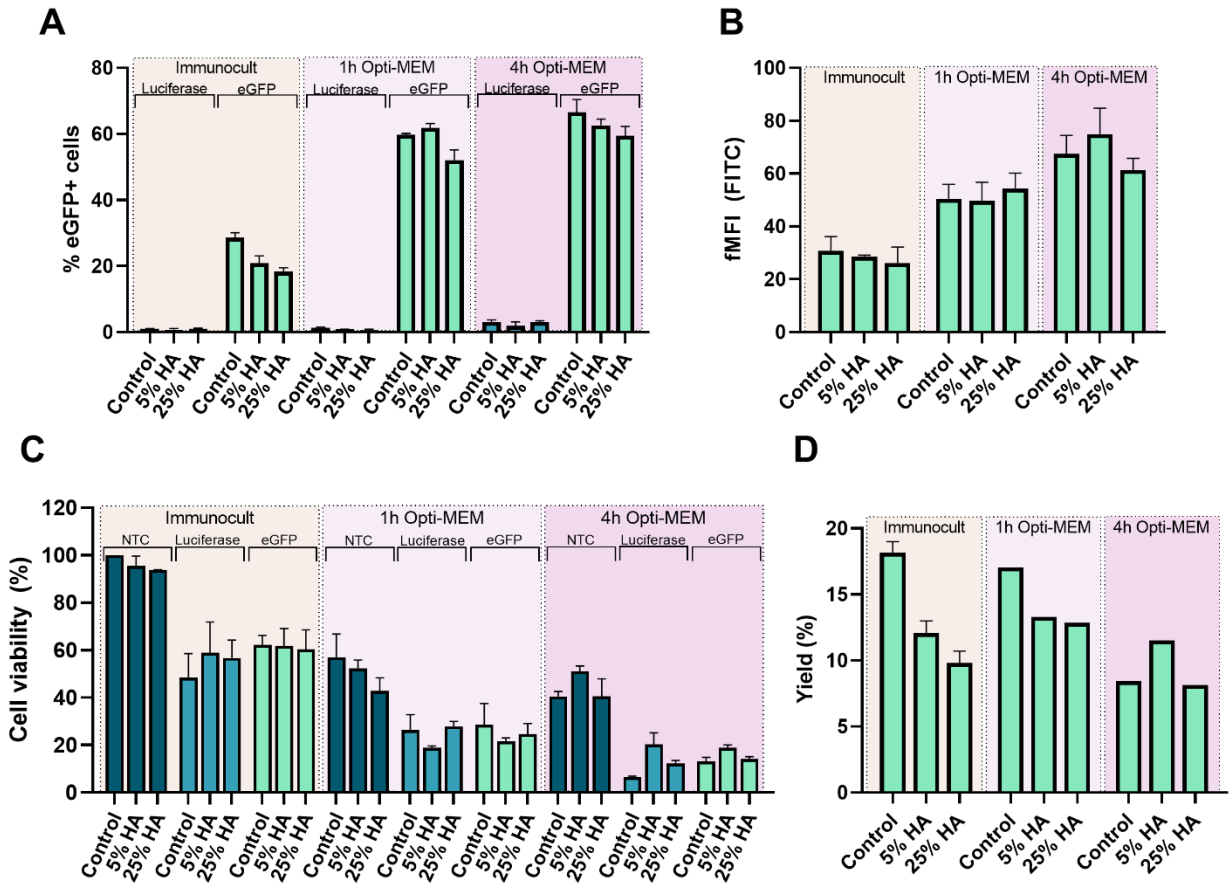


***Figure 7.*** *Analysis of transfection efficiency and cytotoxicity of HA-coated DOTAP LNPs after 1 and 4 hours incubation in Opti-MEM.* ***A-B)*** *Percentage and fMFI of eGFP-positive cells after transfection.* ***C)*** *Cell viability of primary T-cells after transfection.* ***D)*** *Yield of viable transfected cells. NTC = Non-Treated Control.*

## 3.6 Decrease in transfection of DOTAP LNPs after HA coating is caused by a decrease in LNP charge

One of the reasons for the relatively high transfection of uncoated DOTAP LNPs is the cationic charge of the LNPs. Although a cause for the cytotoxicity of DOTAP LNPs as well, the charge allows for strong interaction with the negatively charged cell membrane and increased LNP uptake and transfection. Accordingly, the switch from a positive to a negative charge after HA coating could be causing a decrease in transfection that masks the potential increasing effect of HA-CD44 interaction. To test this hypothesis, DOTAP LNPs were formulated and coated with poly(sodium 4-styrenesulfonate) (PSS). While this coating simulates the change in charge after HA coating, it lacks the ability to interact with CD44, which allows for distinction between the effect of the change in charge and the effect of HA-CD44 interaction. First, a range of PSS coating concentrations was tested to be able to acquire PSS-coated LNPs with a comparable charge to the HA-coated LNPs (*Tab. 7*). Overall, PSS gave stronger anionic charged than HA, probably due to size difference, as the used HA and PSS are 20 and 70 kDa, respectively. 2% and 10% of PSS were chosen as coating concentrations, as the charges of LNPs coated with these concentrations seemed to correspond to the charges of 5% and 25% HA coated LNPs.

Regarding transfection efficiency, PSS coating with 2% and 10% PSS had a strong negative. Whereas HA coating caused a small decrease in transfection compared to uncoated DOTAP LNPs, PSS coating completely blocked transfection (*Fig. 8A*). Interestingly, even the percentage of LNP-positive cells, which has been 100% in all conditions in previous transfections, decreased to around 80% in the PSS-coated conditions (*Fig. 8B*). Unfortunately, a valid conclusion cannot be drawn from this transfection

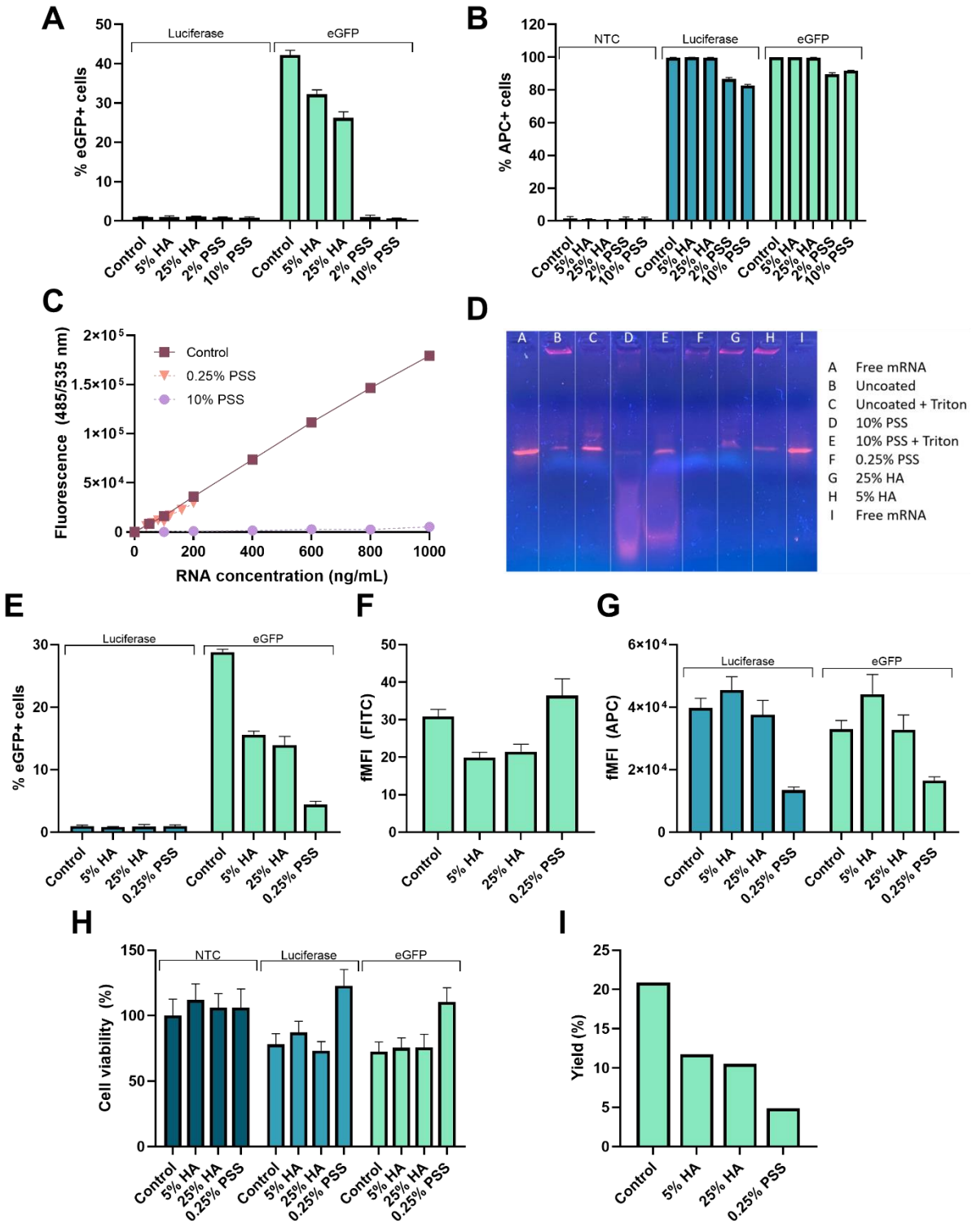


***Figure 8.*** *Analysis of transfection efficiency and cytotoxicity of PSS-coated DOTAP LNPs.* ***A-B)*** *Percentage of eGFP- and LNP-positive cells after transfection with DOTAP LNPs coated with 2% and 10% PSS.* ***C)*** *Ribogreen-PSS interaction test.* ***D)*** *Gel electrophoresis results of PSS- and HA-coated LNPs with and without Triton-X100 treatment.* ***E-F)*** *Percentage and fMFI of eGFP-positive cells after transfection with 0.25% PSS-coated LNPs.* ***G)*** *fMFI of LNP-positive cells.* ***D)*** *Cell viability of primary T-cells after transfection.* ***E)*** *Yield of viable transfected cells. NTC = Non-Treated Control.*

since the amount of mRNA in the PSS-coated LNPs is uncertain. During characterisation, the Ribogreen assay for mRNA concentration gave abnormal values for all PSS-coated LNPs, preventing a reliable quantification of the encapsulated mRNA (*Tab. S2*). Accordingly, the lack of transfection in the PSS-coated LNPs could simply be due to a lack of mRNA. Even so, the decrease in uptake is a promising indication that charge decrease indeed strongly affects uptake and transfection efficiency.

***Table 7.*** *Size, PDI and charge of empty DOTAP formulations with various PSS coating concentrations. Concentration of PSS is expressed as molar percentage of the total amount of DOTAP moles.*

| LNP | Size (nm) | PDI | Zeta potential |
|---|---|---|---|
| **Control** | 89,1 ± 3,93 | 0,405 ± 0,03 | 17,9 ± 0,42 |
| **2% PSS** | 101,6 ± 3,76 | 0,340 ± 0,01 | -21,0 ± 1,44 |
| **5% PSS** | 78,9 ± 5,53 | 0,293 ± 0,02 | -22,8 ± 0,86 |
| **10% PSS** | 73,8 ± 0,96 | 0,200 ± 0,01 | -26,0 ± 2,16 |
| **25% PSS** | 89,7 ± 2,81 | 0,266 ± 0,01 | -28,2 ± 0,70 |
| **50% PSS** | 94,7 ± 2,21 | 0,352 ± 0,02 | -36,1 ± 2,68 |

To discover the cause of these abnormal values in the Ribogreen assay, several tests were performed. First, an RNA standard curve supplemented with 10% PSS was measured with Ribogreen reagent to reveal any possible interaction of PSS with the reagent. If no such interaction exists, a standard curve with PSS should be identical to a standard curve without PSS. Second, mRNA in PSS- and HA-coated LNPs was visualised with gel electrophoresis to test if DOTAP LNPs remain intact when coated with PSS. In gel electrophoresis, mRNA encapsulated in LNPs remains at the top as the LNPs cannot diffuse through the gel, while free mRNA diffuses downwards through the gel. If LNPs coated with PSS remain intact, most mRNA should be encapsulated and visualised at the top of the gel. The results show that PSS at a concentration of 10% both interacts with the Ribogreen reagent (*Fig. 8C*), and causes mRNA to be released from the LNPs (*Fig. 8D*), which makes reliable quantification of mRNA in LNPs with 10% PSS impossible. Additionally, RNA seems to be degraded in the presence of 10% PSS, as demonstrated by the smear of RNA in the presence of 10% PSS instead of a clear band (*Fig. 8D*).

Besides 10% PSS, a lower PSS concentration was tested as well. At 0.25% PSS, interaction with the Ribogreen reagent is very low, especially in the low RNA concentration range where our LNPs are normally situated (*Fig. 8C*). When DOTAP LNPs were coated with 0.25% PSS, charge remained comparable to 5% HA-coated LNPs, and the Ribogreen assay seemed to provide normal values (*Tab. S3*). When performing gel electrophoresis, almost no RNA in the 0.25% PSS LNPs was visible in the lower part of the gel, which suggests that the LNPs stay mainly intact (*Fig. 8D*). However, the intensity of the mRNA band at the top of the gel is lower for 0.25% PSS compared to 5% and 25% HA. Since the loading calculation was based on the Ribogreen assay, it is likely that the Ribogreen assay with 0.25% PSS is thus far not completely reliable. Nevertheless, it can be concluded that at 0.25% PSS, most mRNA remains encapsulated within the LNPs. Therefore, 0.25% PSS coating was tested in transfection as well.

Although transfection was not completely blocked by coating with 0.25% PSS as it was with 10% PSS, it was still extremely low (*Fig. 8E*). The fMFI of PSS-coated LNPs was higher than HA-coated LNPs (*Fig. 8F*). This is because the autofluorescence, and thus overall MFI of the whole population, was much lower. Since fMFI is the ratio of MFI of the positive population over the overall MFI of the control (luciferase) condition, a lower overall MFI will give a higher fMFI, even though transfection might actually be lower. Besides transfection efficiency, uptake was clearly affected as well. Although the percentage of LNP-positive cells remained at 100% (*Fig. S1E*), fMFI of 0.25% PSS was less than half of the other conditions (*Fig. 8G*). Interestingly, PSS coating was able to shield the cells completely from cytotoxicity, which was originally expected from HA coating as well. However, even with the high cell viability, the yield of the PSS-coated LNPs was less than half of the HA-coated conditions. Notably, the

amount of mRNA added to the T-cells in the PSS-coated condition might be slightly lower due to the unreliable Ribogreen assay. Nonetheless, PSS-coated LNPs have a distinctly different effect from uncoated and HA-coated LNPs in parameters unaffected by RNA as well, such as uptake and cytotoxicity. Overall, it can be concluded that a change from cationic to anionic charge strongly affects the uptake, cytotoxicity, and transfection efficiency of LNPs on T-cells. Since the charge of the PSS- and HA-coated LNPs was comparable, the charge-dependent decrease in transfection after coating should be comparable for both HA and PSS as well. The large difference in transfection efficiency between the PSS- and HA-coated LNPs indicates that the hypothesized interaction of CD44 with HA does contribute in some way to the increase in transfection efficiency compared to negatively charged PSS-coated LNPs.

## 3.7 Electrostatic HA-coating does not decrease transfection of neutrally charged C12-200 LNPs

To test the effect of HA-coating on transfection without the charge switch from cationic to anionic, another LNP with neutral charge was coated and tested for transfection efficiency on T-cells. The used LNP formulation, C12-200, is similar in composition to the DOTAP LNPs, but lacks the cationic DOTAP lipid. This yields an LNP that is cationic in acidic solution, but neutral at a physiological pH. Surprisingly, the electrostatic coating method used for the cationic DOTAP LNPs yielded strongly anionic C12-200 LNPs as well (*Tab. 8*), even though electrostatic interaction should not be possible without cationic charge. Possibly another type of interaction is responsible for the coating. Encapsulation efficiency of C12-200 LNPs was slightly lower than the DOTAP LNPs, and decreased even more with HA coating. This decrease in encapsulation efficiency after coating was not seen in DOTAP LNPs, which fortifies the hypothesis that another type of interaction occurs between HA and C12-200 LNPs.

***Table 8.*** *Size, PDI, charge, and encapsulation efficiency of C12-200 LNPs coated with 5% and 25% HA*

| LNP | Size (nm) | PDI | Zeta potential | Encapsulation efficiency (%) |
|---|---|---|---|---|
| **Control** | 145,7 ± 14,03 | 0,234 ± 0,03 | 9,7 ± 0,78 | 93,0 ± 0,50 |
| **5% HA** | 160,7 ± 11,78 | 0,204 ± 0,08 | -12,4 ± 1,94 | 82,2 ± 1,95 |
| **25% HA** | 165,0 ± 13,15 | 0,223 ± 0,07 | -15,1 ± 2,44 | 82,0 ± 0,83 |

Since the type of coating interaction is unknown, the stability of the coating was tested with FCS in HEPES and ImmunoCult™-XF (*Fig. 9*). Similar to the HA-coated DOTAP LNPs, a lot of free HA was present, but many peaks were measured as well. Additionally, the peaks were measured in ImmunoCult™-XF with similar height and amount, which indicates the coating is quite stable and can be used for transfection.

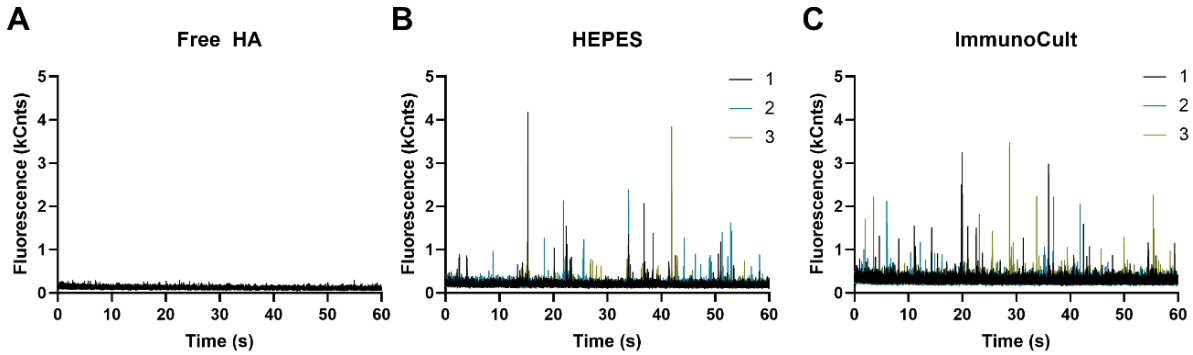


***Figure 9.*** *FCS results of C12-200 LNPs coated with HA-Cy5 in HEPES buffer and ImmunoCult™-XF.* ***A)*** *Free HA-Cy5 in HEPES buffer.* ***B)*** *C12-200 LNPs with 5% HA-Cy5 in HEPES buffer.* ***C.*** *C12-200 LNPs with*

*5% HA-Cy5 in ImmunoCult™-XF after 4 hours incubation at 37 °C. Numbers in legend represent technical replicates.*

For C12-200 LNPs, a distinctly different effect of HA coating could be seen from HA coating on DOTAP LNPs regarding transfection efficiency. Whereas a consistent decrease in transfection was seen after HA coating on DOTAP LNPs, transfection level remained stable after HA coating of C12-200 LNPs (*Fig. 10A-B*). HA-coated C12-200 transfection was performed on T-cells from two different donors. Interestingly, in one of the donors a small increase in transfection was seen after coating. Additionally, uptake seemed to increase slightly as well (*Fig. 10C*). Cytotoxicity of the neutral C12-200 LNPs is much lower than the cationic DOTAP LNPs (*Fig. 10D*). Only around 10% of cell viability was lost in the C12-200 transfected conditions compared to the non-treated controls. HA coating did not affect the cytotoxicity of the C12-200 LNPs. Overall, the yield was comparable for uncoated and HA-coated C12-200 LNPs (*Fig. 10E*). On the whole, this transfection shows that HA coating has vastly different effects on cationic and neutral LNPs, confirming that LNP charge plays a crucial role in transfection efficiency on T-cells. While the cationic DOTAP LNPs consistently decreased in transfection efficiency after a HA coating switched the overall cationic charge to anionic, the neutral C12-200 LNPs kept a similar transfection level, as transfection efficiency of C12-200 was never reliant on a positive charge. Unfortunately, no clear increase can be seen after HA coating of C12-200 LNPs either. In one of the T-cell donors, there seems to be a very small increase in transfection, uptake and yield after HA coating. However, this difference is too small to draw conclusions. Nevertheless, some hope can be drawn from this transfection that with extensive optimisation, a benefit of HA coating might still be seen on the transfection of primary T-cells.

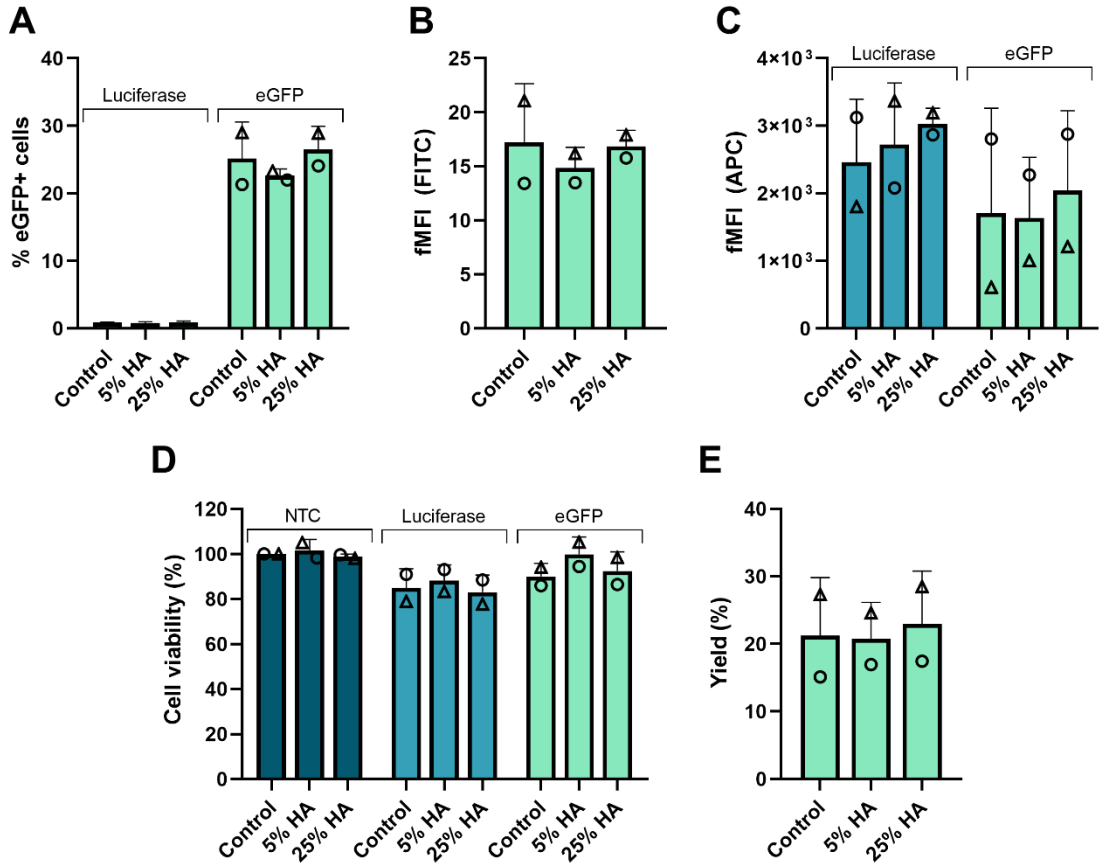


***Figure 10.*** *Analysis of transfection efficiency and cytotoxicity of HA-coated C12-200 LNPs on primary T-cells.* ***A-B)*** *Percentage and fMFI of eGFP-positive cells after transfection.* ***C)*** *fMFI of LNP-positive cells.* ***D)*** *Cell viability of primary T-cells after transfection.* ***E)*** *Yield of viable transfected cells. Data represents biological replicates (N=2). NTC = Non-Treated Control.*

# 4 Discussion

In this report, we showed that HA does not increase the transfection efficiency of cationic DOTAP LNPs on T-cells. Instead, transfection efficiency of DOTAP LNPs clearly decreases after HA coating. Additionally, a reduction in cytotoxicity of the LNPs could not be obtained. By formulating and coating DOTAP LNPs with decreased PEGylated lipid presence, we demonstrated that the presence of PEG does not influence the effect of HA coating on transfection, verifying that PEG does not interfere in HA-LNP interaction. Although we were unable to validate specific binding of HA to the CD44 receptor, the titration with fluorescently labelled HA showed a strong dose-dependent binding to the T-cells, suggesting that the lack of increased transfection was not due to inability of HA to bind to the T-cells. Use of conjugated HA-DOPE for coating had the same effect on transfection efficiency as electrostatically coated LNPs. However, coating method was suboptimal for conjugate coating, and likely not representative of a stable conjugate coating. Due to an excess of free HA present in our LNP solutions, it was not possible to quantify stability of the HA coating in medium with FCS. Visual examination revealed that peaks of LNPs incubated in ImmunoCult™-XF were slightly lower compared to HEPES and Opti-MEM, suggesting some loss of coating. However, the more stable HA-coating in Opti-MEM did not translate into increased transfection efficiency compared to uncoated LNPs. Overall transfection was higher in Opti-MEM, but decreased with HA coating as well, showing that coating stability and cell culture medium do not play a role in the effect of HA coating. By coating DOTAP LNPs with PSS, we showed that LNPs coated with another negatively charged polymer with no interaction with CD44 had an even bigger decrease in transfection efficiency compared to HA coated LNPs, suggesting that the switch from a cationic to an anionic LNP contributes to the decrease in transfection efficiency after HA coating. Accordingly, HA coating on neutral C12-200 LNPs that do not rely on cationic charge for transfection did not decrease the transfection efficiency of the LNPs. Unfortunately, even without the charge-dependent decrease, HA coating did not increase the transfection efficiency of the C12-200 LNPs, indicating that other factors interfere as well. Overall, we showed that HA coating offers no benefit in terms of transfection efficiency and cell viability of primary T-cells in the investigated conditions.

Although this was the first time HA coating was tested for the transfection of primary T-cells, HA coating of particles has been tested in several other contexts before, ranging from retinal to cancer cells, from liposomes to polymeric particles, from conjugate to electrostatic coating, and from less than 10 kDa up to 1.600 kDA sizes of HA.[53-62] Two previously published studies describe electrostatic coating of cationic lipoplexes containing DOTAP lipids, used for transfection of retinal cells and monocytes.[55,57] In both cases, no effect was found on transfection efficiency. Interestingly, when a conjugate HA coating was used on the same lipoplex, an 8-fold increase in transfection of retinal cells was found.[57] In a different ocular cell line, electrostatic coating of cationic polymeric particles increased transfection dose-dependently when a larger size HA was used.[53] In cancer research, delivery with HA-coated particles is tested mainly on CD44-overexpressing cell lines with electrostatically coated cationic polymeric or lipid nanoparticles. In all cases, transfection was increased after HA coating.[58-62] Additionally, electrostatic coating of PEI-DNA complexes restored cell viability up to the level of untreated cells.[61] Conjugated HA coating was tested on drug-delivering liposomes in macrophages and lung cells.[54,56] Delivery and uptake was increased in both cases. Our study provides the first information about the effect of HA coating for T-cell transfection. Although we did not show beneficial effect, we gained valuable knowledge about the different factors influencing the effect of HA coating that have not been explicitly shown before.

Overall, our study comprises several strong points. The use of primary T-cells reinforces the relevancy of our experiments, since it is a close resemblance of clinical CAR T-cell production. Hence, the results closely reflect how our parameters would affect CAR T-cell generation the clinic, including biological

variation between different T-cell donors. In total, many different parameters were tested for their role in the transfection, which allowed elimination of several possible causes for the decreased transfection. In all experiments, proper controls were used to distinguish between relevant effects and error-induced artefacts.

Yet besides strengths, several challenges were encountered as well, in which we were limited by time and the availability of materials and methods. In the HA-FITC titration to determine the binding of HA to CD44 on T-cells, CD44 blocking with anti-CD44 did not give conclusive results, because it is unknown if the used anti-CD44 completely blocks the HA binding epitope. An alternative approach to provide an elimination of CD44 on T-cells is the use of siRNA to obtain a knock-down of CD44 expression. Unfortunately, CD44 encoding siRNA was not available to perform these experiments. Furthermore, during stability testing of the HA coating with FCS, it was discovered that an excess of free HA was present in our LNP solutions, preventing quantification of the association and dissociation of our HA coating. Therefore, no clear conclusion can be drawn about the amount of coating on the LNPs and possible coating loss in cell culture medium besides showing some HA-coated LNPs were present in all conditions. Removal of the excess free HA with ultracentrifugation or size-based centrifuge filters would solve this problem. Unfortunately, this was not feasible with the available time and methods. Further, PSS, the anionic polymer used to test the effect of charge, had an unexpected interaction with both the Ribogreen reagent and the LNPs. The effect was minimised by lowering PSS coating concentrations, but the exact amount of mRNA used for transfection in this condition is still unknown. Despite this uncertainty, overall effect of PSS-coated LNPs was sufficiently distinct from HA-coated LNPs regarding parameters unaffected by RNA, which allows for drawing a reliable conclusion. Lastly, large variation in overall transfection efficiency was found between the different donors, hindering comparison and statistical significance. However, the relative effect of the various HA and PSS coatings was consistent in all donors. All-in-all, many of the experiments had some weakness which diminished the conclusion. Nevertheless, influence of these limitations was minimised where possible with additional control experiments and alternative parameters, allowing for reliable conclusions to be drawn.

The lack of benefit of HA coating was an unexpected finding, considering the abundant literature reporting the opposite. It was clearly shown by the decrease in transfection after PSS coating and the lack of decreasing transfection after HA coating of neutral LNPs that a charge switch was the main culprit for decreasing transfection of HA-coated DOTAP LNPs. In literature, electrostatic HA-coating on cationic particles often did increase transfection. However, in most cases, a HA coating concentration was used in which the overall charge of the particles actually remained cationic even after coating.[58,59,61] Moreover, when an anionic and cationic HA-coated complex were compared, the cationic formulation with less HA coating had a substantially higher transfection compared to the anionic formulation with more HA.[61] Similarly, in both studies in which electrostatic HA coating did not increase transfection of DOTAP lipoplexes, HA coating concentrations leading to anionic particle charge were used. Overall, literature seems to confirm the importance of charge in the effect of HA coating, yet reports of anionic HA-coated LNPs improving transfection can be found as well.[53] Possibly, some cells are more sensitive to the effect of charge, leading to the diverse effects. Several studies report a cationic charge leads to strongly improved delivery to T-cells, with varying effects on cell viability, suggesting charge greatly affects transfection of T-cells.[66-68]

Besides transfection, HA coating did not affect the cytotoxicity of DOTAP LNPs. A possible cause is loss of the shielding effect after LNP uptake. If the cationic DOTAP lipid and anionic HA are separated during the uptake and endosomal release process, the shielding effect of HA would disappear, exposing the cell to the cationic DOTAP. However, this is a hypothesis and no experiments were done to verify this.

After electrostatic coating of the C12-200 LNPs, transfection did not go down, yet transfection did not increase either. As can be seen in literature, many parameters can influence the effect of HA coating and could be contributing to this lack of increased transfection. Most likely, a main contributor is the presence of free HA. During stability experiments with FCS, it was discovered that a large part of the added HA does not coat the LNPs, but instead remains free. This free HA is not removed from the LNPs after coating, and remains present in the solution. During transfection, the free HA can interact with CD44 on the T-cells, which blocks the receptor and prevents the HA-LNPs from binding. In two separate studies, it was shown that HA-induced improvement in delivery of nanoparticles was completely blocked by pre-treatment of cells with free HA.[58,59] Nevertheless, other factors likely contribute as well. It is known that the size of HA can strongly affect binding affinity to CD44. Binding affinity of free HA to the CD44 receptor increases with increasing HA size until saturation is reached around 200-300 kDa.[69,70] Moreover, binding and uptake of HA-coated particles increases as well with a larger size of HA.[70,71] Additionally, intracellular particle presence is sustained for a longer time with larger HA sizes.[72] In all all our experiments, a relatively small HA of 20 or 50 kDa was used, which means the affinity of the HA for CD44 could be too small to see an effect in delivery. For future experiments, the optimal HA size for improving transfection could be determined by comparing HA-coated particles with HA sizes between 50 and 200 kDa. Besides HA size, the method of coating can also influence the results. Where electrostatic coating might have no effect on a particle, conjugate coating of the same particle can greatly increase transfection.[57] Especially since the type of interaction responsible for the HA coating on the neutral C12-200 LNP is unknown, it could be that the coating method used is simply not compatible with HA-LNP-CD44 interaction. Lastly, CD44 receptor internalisation, which is needed for CD44-mediated improvement in transfection, has not been shown on T-cells. While CD44 is known to internalise on tumour cell lines, chondrocytes, fibroblasts, and macrophages, it is possible that a lack of internalisation on T-cells contributes to the lack of improved transfection efficiency.[73-75] Therefore, CD44 internalisation upon ligand binding should be validated in T-cells with the use of CD44 labelling and confocal microscopy.

If transfection of primary T-cells is improved by HA coating, it could contribute to the development of CAR T-cells without viral vector, which would be both safer and more accessible due to lower costs and production time. Since we were not able to improve transfection, our results are not directly relevant to the clinic. However, a great deal of information can be found in our data. We showed that in primary T-cells, the presence of PEGylated lipids does not prevent binding of HA-LNPs to CD44. With FCS ,we demonstrated that electrostatic coating of cationic LNPs is stable in cell culture medium, and that proteins in the medium do not interfere in the binding of HA-LNPs to CD44. Lastly, we showed that a decrease in charge can strongly decrease transfection of cationic LNPs, and that the presence of free HA can most likely block any beneficial effect of HA-coated LNPs. With this information, new studies can be designed to optimise HA coating of LNPs for T-cell transfection, which might eventual yield LNPs with high T-cell transfection for CAR T-cell generation.

All-in-all, we showed that electrostatic HA coating of cationic DOTAP LNPs decreased transfection of primary T-cells, while cytotoxicity of the LNPs remained the same. The drop in transfection is likely caused by the switch from cationic to anionic LNPs. The lack of reduced cytotoxicity might be because the HA and DOTAP are separated after uptake, which negates the shielding effect. Electrostatic coating of neutral C12-200 LNPs did not decrease transfection, but also did not increase it. Most likely, an excess of free HA in the solution is binding the CD44 receptor and blocking receptor-mediated endocytosis of the HA-LNPs. In future experiments, results might be improved by switching to a conjugate coating method of C12-200 LNPs in which excess HA is removed, as well as increasing the size of HA. Alternatively, a different targeting ligand such as antibodies or nanobodies could be used to target T-cells via CD44. To conclude, we provided valuable information about the different parameters

influencing transfection efficiency of HA-coated LNPs, bringing us one step closer to efficient LNP-mediated T-cell transfections for safer and more accessible CAR T-cell therapy.

# 5 Acknowledgements

First and foremost, I would like to thank Laure Harinck for supervising me in my lab work. You taught me new techniques with patience and extensive explanations, and improved my existing skills. On top of that, you always made me feel welcome and were there whenever I needed help.

I would also like to thank Koen Raemdonck, for giving me the opportunity to work in his lab and taking the time to guide my project, and Raymond Schiffelers, for being my examiner in Utrecht.

Next, I would like to thank everyone at the lab. Everyone was very friendly and inclusive, and was always willing to help when needed.

Last, I would like to give a special thanks to Anna Cielo. Sharing an office with you made my days, and I am forever grateful for your friendship.

# 6 References


1. Zhang P, Zhang G, Wan X. Challenges and new technologies in adoptive cell therapy. *Journal of Hematology & Oncology*. 2023;16(1):1-55.

2. Köhl U, Arsenieva S, Holzinger A, Abken H. CAR T cells in trials: Recent achievements and challenges that remain in the production of modified T cells for clinical applications. *Hum Gene Ther*. 2018;29(5):559-568. doi: 10.1089/hum.2017.254.

3. Rose S. First-ever CAR T-cell therapy approved in U.S. *Cancer Discov*. 2017;7(10):OF1. doi: 10.1158/2159-8290.CD-NB2017-126.

4. Jommi C, Bramanti S, Pani M, Ghirardini A, Santoro A. CAR T-cell therapies in italy: Patient access barriers and recommendations for health system solutions. *Front Pharmacol*. 2022;13:915342. doi: 10.3389/fphar.2022.915342.

5. Gill S, Maus MV, Porter DL. Chimeric antigen receptor T cell therapy: 25years in the making. *Blood Rev*. 2016;30(3):157-167. doi: 10.1016/j.blre.2015.10.003.

6. Khalil DN, Smith EL, Brentjens RJ, Wolchok JD. The future of cancer treatment: Immunomodulation, CARs and combination immunotherapy. *Nat Rev Clin Oncol*. 2016;13(5):273-290. doi: 10.1038/nrclinonc.2016.25.

7. Kymriah: EPAR - product information. *European Medicine Agency*. 2023.

8. Carvykti: EPAR - product information. *European Medicine Agency*. 2023.

9. Abecma: EPAR - product information. *European Medicine Agency*. 2022.

10. Breyanzi: EPAR - product information. *European Medicine Agency*. 2022.

11. Tecartus: EPAR - product information. *European Medicine Agency*. 2023.

12. Yescarta: EPAR - product information. *European Medicine Agency*. 2023.

13. Luciw PA, Leung NJ. Mechanisms of retrovirus replication. *The Retroviridae*. 1992:159-298. doi: 10.1007/978-1-4615-3372-6_5.

14. Topp M, Feuchtinger T. Management of hypogammaglobulinaemia and B-cell aplasia. In: Kröger N, Gribben J, Chabannon C, Yakoub-Agha I, Einsele H, eds. *The EBMT/EHA CAR-T cell handbook.* Cham (CH): Springer; 2022. http://www.ncbi.nlm.nih.gov/books/NBK584138/. Accessed May 25, 2023.

15. Shimabukuro-Vornhagen A, Gödel P, Subklewe M, et al. Cytokine release syndrome. *Journal for immunotherapy of cancer*. 2018;6(1):1-14.

16. Xiao X, Huang S, Chen S, et al. Mechanisms of cytokine release syndrome and neurotoxicity of CAR T-cell therapy and associated prevention and management strategies. *J Exp Clin Cancer Res*. 2021;40(1):367. doi: 10.1186/s13046-021-02148-6.

17. Gorovits B, Koren E. Immunogenicity of chimeric antigen receptor T-cell therapeutics. *BioDrugs*. 2019;33(3):275-284. doi: 10.1007/s40259-019-00354-5.

18. David RM, Doherty AT. Viral vectors: The road to reducing genotoxicity. *Toxicol Sci*. 2016;155(2):315-325. doi: 10.1093/toxsci/kfw220.

19. Hacein-Bey-Abina S, Garrigue A, Wang GP, et al. Insertional oncogenesis in 4 patients after retrovirus-mediated gene therapy of SCID-X1. *J Clin Invest*. 2008;118(9):3132-3142. doi: 10.1172/JCI35700.

20. Billingsley MM, Singh N, Ravikumar P, Zhang R, June CH, Mitchell MJ. Ionizable lipid nanoparticle-mediated mRNA delivery for human CAR T cell engineering. *Nano Lett*. 2020;20(3):1578-1589. doi: 10.1021/acs.nanolett.9b04246.

21. Scudellari M. Attack of the killer clones. *Nature*. 2017;552(7685):S64-S66. doi: 10.1038/d41586-017-08701-8.

22. Sweeney NP, Vink CA. The impact of lentiviral vector genome size and producer cell genomic to gag-pol mRNA ratios on packaging efficiency and titre. *Mol Ther Methods Clin Dev*. 2021;21:574-584. doi: 10.1016/j.omtm.2021.04.007.

23. Borgert R. Improving outcomes and mitigating costs associated with CAR T-cell therapy. *Am J Manag Care*. 2021;27(13 Suppl):S253-S261. doi: 10.37765/ajmc.2021.88737.

24. Patient access analytics. Ori Biotech Web site. https://oribiotech.com/patient-access-analytics/. Updated 2023. Accessed Sep 19, 2023.

25. Guevara ML, Persano F, Persano S. Advances in lipid nanoparticles for mRNA-based cancer immunotherapy. *Front Chem*. 2020;8:589959. doi: 10.3389/fchem.2020.589959.

26. Pastor F, Berraondo P, Etxeberria I, et al. An RNA toolbox for cancer immunotherapy. *Nat Rev Drug Discov*. 2018;17(10):751-767. doi: 10.1038/nrd.2018.132.

27. Barrett DM, Zhao Y, Liu X, et al. Treatment of advanced leukemia in mice with mRNA engineered T cells. *Hum Gene Ther*. 2011;22(12):1575-1586. doi: 10.1089/hum.2011.070.

28. Harrer DC, Simon B, Fujii S, et al. RNA-transfection of γ/δ T cells with a chimeric antigen receptor or an α/β T-cell receptor: A safer alternative to genetically engineered α/β T cells for the immunotherapy of melanoma. *BMC Cancer*. 2017;17:551. doi: 10.1186/s12885-017-3539-3.

29. Svoboda J, Rheingold SR, Gill SI, et al. Nonviral RNA chimeric antigen receptor-modified T cells in patients with hodgkin lymphoma. *Blood*. 2018;132(10):1022-1026. doi: 10.1182/blood-2018-03-837609.

30. Rabinovich PM, Komarovskaya ME, Ye Z, et al. Synthetic messenger RNA as a tool for gene therapy. *Hum Gene Ther*. 2006;17(10):1027-1035. doi: 10.1089/hum.2006.17.1027.

31. Zhao Y, Moon E, Carpenito C, et al. Multiple injections of electroporated autologous T cells expressing a chimeric antigen receptor mediate regression of human disseminated tumor. *Cancer Res*. 2010;70(22):9053-9061. doi: 10.1158/0008-5472.CAN-10-2880.

32. Singh N, Liu X, Hulitt J, et al. Differences in control of local versus disseminated neuroblastoma by transiently-modified GD2 CAR T cells due to variability in tumor penetration. *Cancer Immunol Res*. 2014;2(11):1059-1070. doi: 10.1158/2326-6066.CIR-14-0051.

33. Tasian SK, Kenderian SS, Shen F, et al. Optimized depletion of chimeric antigen receptor T cells in murine xenograft models of human acute myeloid leukemia. *Blood*. 2017;129(17):2395-2407. doi: 10.1182/blood-2016-08-736041.

34. Foster JB, Choudhari N, Perazzelli J, et al. Purification of mRNA encoding chimeric antigen receptor is critical for generation of a robust T-cell response. *Hum Gene Ther*. 2019;30(2):168-178. doi: 10.1089/hum.2018.145.

35. Beatty GL, Haas AR, Maus MV, et al. Mesothelin-specific chimeric antigen receptor mRNA-engineered T cells induce anti-tumor activity in solid malignancies. *Cancer Immunol Res*. 2014;2(2):112-120. doi: 10.1158/2326-6066.CIR-13-0170.

36. Yoon SH, Lee JM, Cho HI, et al. Adoptive immunotherapy using human peripheral blood lymphocytes transferred with RNA encoding her-2/neu-specific chimeric immune receptor in ovarian cancer xenograft model. *Cancer Gene Ther*. 2009;16(6):489-497. doi: 10.1038/cgt.2008.98.

37. DiTommaso T, Cole JM, Cassereau L, et al. Cell engineering with microfluidic squeezing preserves functionality of primary immune cells in vivo. *Proc Natl Acad Sci U S A*. 2018;115(46):E10907-E10914. doi: 10.1073/pnas.1809671115.

38. Onpattro: EPAR - product information. *European Medicine Agency*. 2023.

39. Billingsley MM, Hamilton AG, Mai D, et al. Orthogonal design of experiments for optimization of lipid nanoparticles for mRNA engineering of CAR T cells. *Nano Lett*. 2022;22(1):533-542. doi: 10.1021/acs.nanolett.1c02503.

40. Rahimmanesh I, Totonchi M, Khanahmad H. The challenging nature of primary T lymphocytes for transfection: Effect of protamine sulfate on the transfection efficiency of chemical transfection reagents. *Res Pharm Sci*. 2020;15(5):437-446. doi: 10.4103/1735-5362.297846.

41. Schlich M, Palomba R, Costabile G, et al. Cytosolic delivery of nucleic acids: The case of ionizable lipid nanoparticles. *Bioeng Transl Med*. 2021;6(2):e10213. doi: 10.1002/btm2.10213.

42. Bhattacharya D, Svechkarev D, Souchek JJ, et al. Impact of structurally modifying hyaluronic acid on CD44 interaction. *J Mater Chem B*. 2017;5(41):8183-8192. doi: 10.1039/C7TB01895A.

43. Garantziotis S, Savani RC. Hyaluronan biology: A complex balancing act of structure, function, location and context. *Matrix Biol*. 2019;78-79:1-10. doi: 10.1016/j.matbio.2019.02.002.

44. Antonio CR, Trídico LA. The importance of interaction between hyaluronic acid and CD44 receptor. *Surgical & Cosmetic Dermatology*. 2021;13(0):1-7. doi: 10.5935/scd1984-8773.2021130006.

45. Laomeephol C, Areecheewakul S, Tawinwung S, et al. Potential roles of hyaluronic acid in in vivo CAR T cell reprogramming for cancer immunotherapy. *Nanoscale*. 2022;14(48):17821-17840. doi: 10.1039/D2NR05949E.

46. Lesley J, Hyman R, English N, Catterall JB, Turner GA. CD44 in inflammation and metastasis. *Glycoconj J*. 1997;14(5):611-622. doi: 10.1023/a:1018540610858.

47. DeGrendele HC, Kosfiszer M, Estess P, Siegelman MH. CD44 activation and associated primary adhesion is inducible via T cell receptor stimulation. *J Immunol*. 1997;159(6):2549-2553.

48. Lesley J, Howes N, Perschl A, Hyman R. Hyaluronan binding function of CD44 is transiently activated on T cells during an in vivo immune response. *J Exp Med*. 1994;180(1):383-387. doi: 10.1084/jem.180.1.383.

49. Galandrini R, Galluzzo E, Albi N, Grossi CE, Velardi A. Hyaluronate is costimulatory for human T cell effector functions and binds to CD44 on activated T cells. *J Immunol*. 1994;153(1):21-31.

50. Ariel A, Lider O, Brill A, et al. Induction of interactions between CD44 and hyaluronic acid by a short exposure of human T cells to diverse pro-inflammatory mediators. *Immunology*. 2000;100(3):345-351. doi: 10.1046/j.1365-2567.2000.00059.x.

51. Jiang Y, Glasstetter LM, Lerman A, Lerman LO. TSG-6 (tumor necrosis factor-α-stimulated gene/protein-6): An emerging remedy for renal inflammation. *Hypertension*. 2022;80(1):35-42.

52. Fröhlich E. The role of surface charge in cellular uptake and cytotoxicity of medical nanoparticles. *Int J Nanomedicine*. 2012;7:5577-5591. doi: 10.2147/IJN.S36111.

53. de la Fuente M, Seijo B, Alonso MJ. Novel hyaluronic acid-chitosan nanoparticles for ocular gene therapy. *Invest Ophthalmol Vis Sci*. 2008;49(5):2016-2024. doi: 10.1167/iovs.07-1077.

54. Bohne Japiassu K, Fay F, Marengo A, et al. Hyaluronic acid-conjugated liposomes loaded with dexamethasone: A promising approach for the treatment of inflammatory diseases. *Int J Pharm*. 2023;639:122946. doi: 10.1016/j.ijpharm.2023.122946.

55. Andretto V, Repellin M, Pujol M, et al. Hybrid core-shell particles for mRNA systemic delivery. *J Control Release*. 2023;353:1037-1049. doi: 10.1016/j.jconrel.2022.11.042.

56. Pandolfi L, Frangipane V, Bocca C, et al. Hyaluronic Acid–Decorated liposomes as innovative targeted delivery system for lung fibrotic cells. *Molecules*. 2019;24(18):3291. doi: 10.3390/molecules24183291.

57. Martens TF, Peynshaert K, Nascimento TL, et al. Effect of hyaluronic acid-binding to lipoplexes on intravitreal drug delivery for retinal gene therapy. *Eur J Pharm Sci*. 2017;103:27-35. doi: 10.1016/j.ejps.2017.02.027.

58. Ma K, Li W, Zhu G, et al. Functionalized PDA/DEX-PEI@HA nanoparticles combined with sleeping-beauty transposons for multistage targeted delivery of CRISPR/Cas9 gene. *Biomed Pharmacother*. 2021;142:112061. doi: 10.1016/j.biopha.2021.112061.

59. Wang T, Hou J, Su C, Zhao L, Shi Y. Hyaluronic acid-coated chitosan nanoparticles induce ROS-mediated tumor cell apoptosis and enhance antitumor efficiency by targeted drug delivery via CD44 | journal of nanobiotechnology | full text. *Journal of Nanobiotechnology*. 2017;15(7).

60. Landesman-Milo D, Goldsmith M, Leviatan Ben-Arye S, et al. Hyaluronan grafted lipid-based nanoparticles as RNAi carriers for cancer cells. *Cancer Lett*. 2013;334(2):221-227. doi: 10.1016/j.canlet.2012.08.024.

61. Sun X, Ma P, Cao X, Ning L, Tian Y, Ren C. Positive hyaluronan/PEI/DNA complexes as a target-specific intracellular delivery to malignant breast cancer. *Drug Deliv*. 2009;16(7):357-362. doi: 10.1080/10717540903059549.

62. Wan T, Pan Q, Liu C, et al. A duplex CRISPR-Cas9 ribonucleoprotein nanomedicine for colorectal cancer gene therapy | nano letters. *Nano Letters*. 2021;21(22):9761-9771.

63. Choi K, Jang M, Kim JH, Ahn HJ. Tumor-specific delivery of siRNA using supramolecular assembly of hyaluronic acid nanoparticles and 2b RNA-binding protein/siRNA complexes. *Biomaterials*. 2014;35(25):7121-7132. doi: 10.1016/j.biomaterials.2014.04.096.

64. Cheng Q, Wei T, Farbiak L, Johnson LT, Dilliard SA, Siegwart DJ. Selective organ targeting (SORT) nanoparticles for tissue-specific mRNA delivery and CRISPR–Cas gene editing. *Nat Nanotechnol*. 2020;15(4):313-320. doi: 10.1038/s41565-020-0669-6.

65. Sandor M, Lynch RG. Lymphocyte fc receptors: The special case of T cells. *Immunol Today*. 1993;14(5):227-231. doi: 10.1016/0167-5699(93)90168-K.

66. Olden BR, Cheng Y, Yu JL, Pun SH. Cationic polymers for non-viral gene delivery to human T cells. *J Control Release*. 2018;282:140-147. doi: 10.1016/j.jconrel.2018.02.043.

67. Rahimmanesh I, Totonchi M, Khanahmad H. The challenging nature of primary T lymphocytes for transfection: Effect of protamine sulfate on the transfection efficiency of chemical transfection reagents. *Res Pharm Sci*. 2020;15(5):437-446. doi: 10.4103/1735-5362.297846.

68. Smith R, Wafa EI, Geary SM, Ebeid K, Alhaj-Suliman SO, Salem AK. Cationic nanoparticles enhance T cell tumor infiltration and antitumor immune responses to a melanoma vaccine. *Sci Adv*. 2022;8(29):eabk3150. doi: 10.1126/sciadv.abk3150.

69. Wolny PM, Banerji S, Gounou C, et al. Analysis of CD44-hyaluronan interactions in an artificial membrane system: Insights into the distinct binding properties of high and low molecular weight hyaluronan. *J Biol Chem*. 2010;285(39):30170-30180. doi: 10.1074/jbc.M110.137562.

70. Mizrahy S, Raz SR, Hasgaard M, et al. Hyaluronan-coated nanoparticles: The influence of the molecular weight on CD44-hyaluronan interactions and on the immune response. *J Control Release*. 2011;156(2):231-238. doi: 10.1016/j.jconrel.2011.06.031.

71. Qhattal HSS, Liu X. Characterization of CD44-mediated cancer cell uptake and intracellular distribution of hyaluronan-grafted liposomes | molecular pharmaceutics. *Mol. Pharmaceutics*. 2011;8(4):1233-1246.

72. Dalla Pozza E, Lerda C, Costanzo C, et al. Targeting gemcitabine containing liposomes to CD44 expressing pancreatic adenocarcinoma cells causes an increase in the antitumoral activity. *Biochim Biophys Acta*. 2013;1828(5):1396-1404. doi: 10.1016/j.bbamem.2013.01.020.

73. Knudson W, Chow G, Knudson CB. CD44-mediated uptake and degradation of hyaluronan. *Matrix Biology*. 2002;21(1):15-23. doi: 10.1016/S0945-053X(01)00186-X.

74. Rios de la Rosa JM, Pingrajai P, Pelliccia M, et al. Binding and internalization in receptor-targeted carriers: The complex role of CD44 in the uptake of hyaluronic acid-based nanoparticles (siRNA delivery). *Adv Healthc Mater*. 2019;8(24):e1901182. doi: 10.1002/adhm.201901182.

75. Aguiar DJ, Knudson W, Knudson CB. Internalization of the hyaluronan receptor CD44 by chondrocytes. *Exp Cell Res*. 1999;252(2):292-302. doi: 10.1006/excr.1999.4641.

# 7 Supplementary data

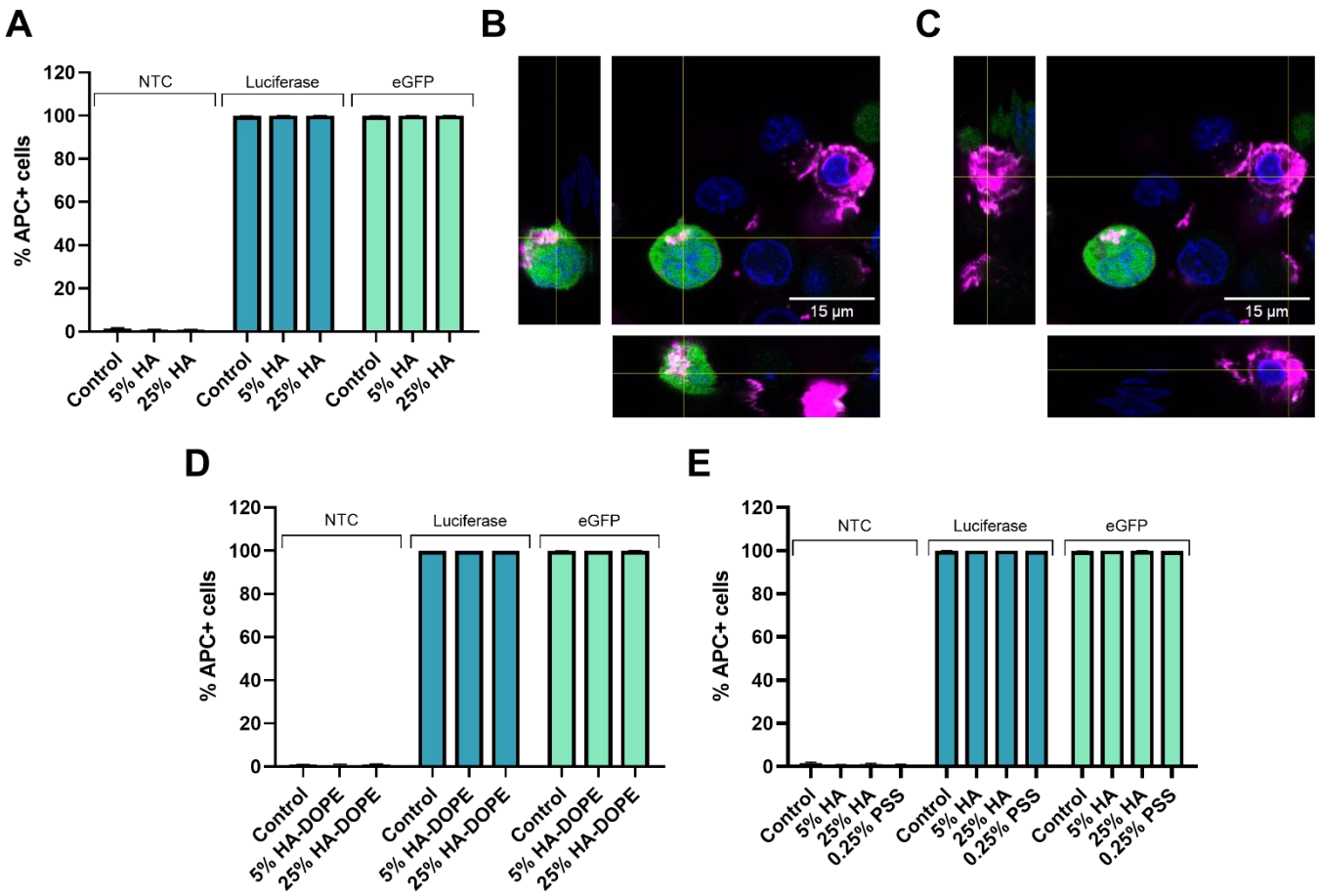


***Figure S1.*** *Analysis of LNP uptake transfection with the various LNPs.* ***A)*** *Percentage of LNP-positive cells after transfection with electrostatically HA-coated DOTAP LNPs. Data represents average of four biological replicates.* ***B-C)*** *Confocal microscopy of primary T-cells transfected with eGFP-containing DOTAP particles. Green = eGFP expression, purple = DiD-labelled LNPs, blue = Hoechst stained nuclei.* ***B)*** *Z-stack overlay of a transfected cell with internalised LNPs.* ***C)*** *Z-stack overlay of untransfected cell.* ***D)*** *Percentage of LNP-positive cells after transfection with DOTAP LNPs coated with conjugated HA-DOPE.* ***E)*** *Percentage of LNP-positive cells after transfection with DOTAP LNPs coated electrostatically with HA and 0.25% PSS.*

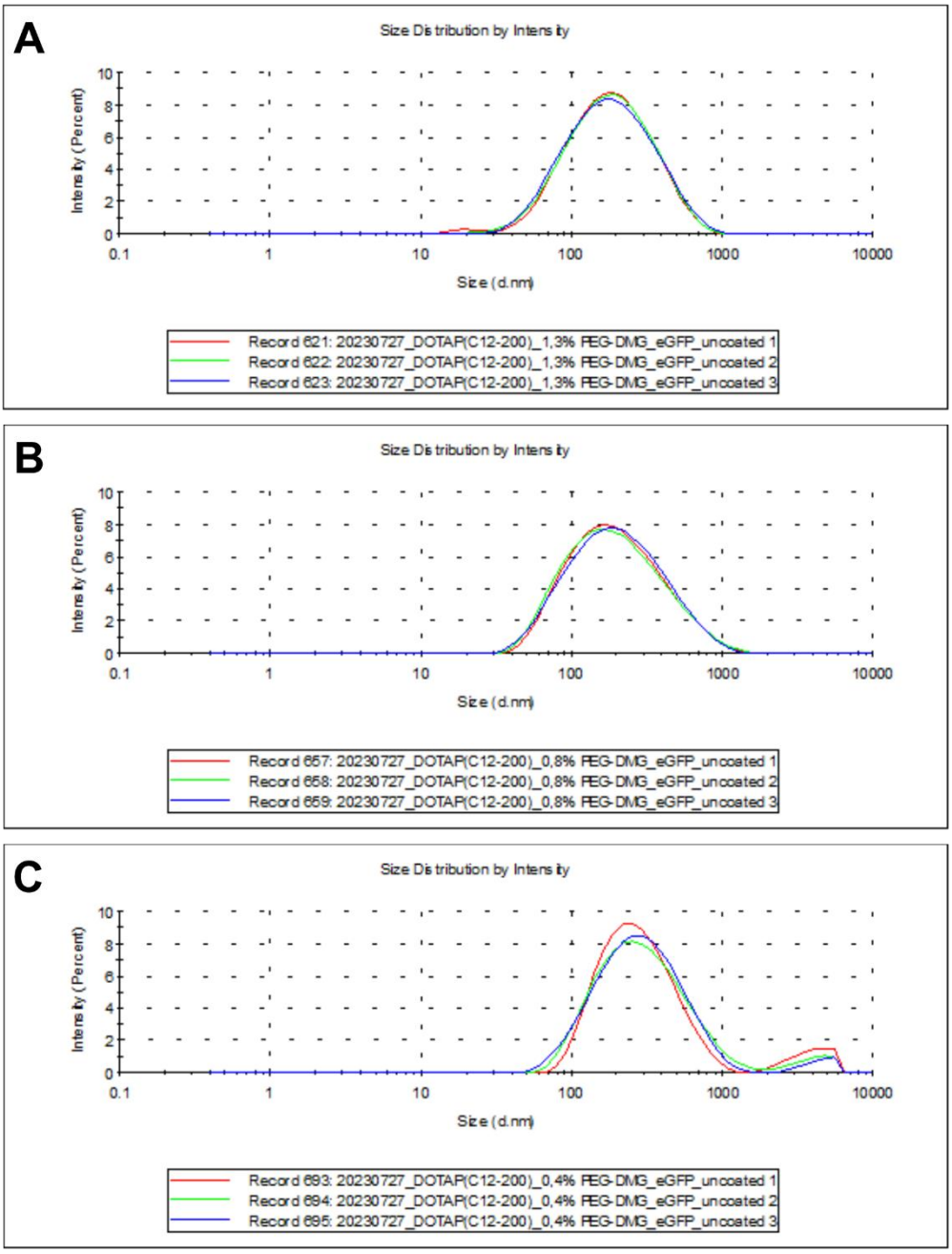


***Figure S2.*** *Results of DLS measurement of uncoated DOTAP LNPs with various PEG-DMG concentrations.* ***A)*** *DOTAP LNP with 1.3% PEG-DMG.* ***B)*** *DOTAP LNP with 0.8% PEG-DMG.* ***C)*** *DOTAP LNP with 0.4% PEG-DMG.*

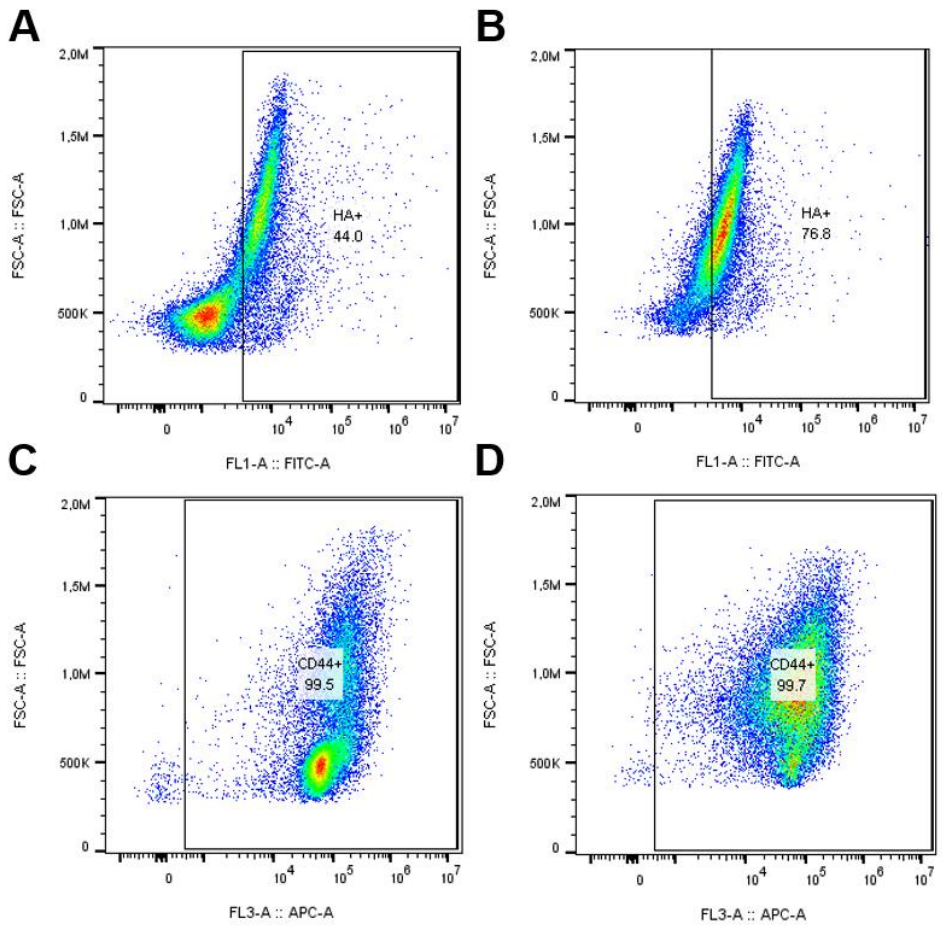


***Figure S3.*** *Flow cytometry dot plots of HA-FITC titration.* ***A)*** *HA-positive cells after incubation with 100 µg/mL HA-FITC on day 3 post-activation.* ***B)*** *HA-positive cells after incubation with 100 µg/mL HA-FITC on day 6 post-activation.* ***C)*** *CD44-positive cells after incubation with anti-CD44 antibody on day 3 post-activation.* ***D)*** *CD44-positive cells after incubation with anti-CD44 antibody on day 6 post-activation.*

***Table S1.*** *Size and PDI of DOTAP LNPs measured in HEPES, ImmunoCult™-XF, and Opti-MEM. LNPs were incubated in ImmunoCult™-XF and Opti-MEM for one hour at 37 °C.*

| LNP | | Size (nm) | PDI |
|---|---|---|---|
| **HEPES** | **Control** | 134,5 ± 2,16 | 0,255 ± 0,01 |
| | **5% HA** | 147,3 ± 2,44 | 0,175 ± 0,03 |
| | **25% HA** | 140,6 ± 3,00 | 0,185 ± 0,02 |
| **ImmunoCult** | **Control** | 245,0 ± 2,35 | 0,767 ± 0,00 |
| | **5% HA** | 46,9 ± 0,25 | 1,000 ± 0,00 |
| | **25% HA** | 44,5 ± 5,33 | 1,000 ± 0,00 |
| **Opti-MEM** | **Control** | 160,0 ± 3,43 | 0,124 ± 0,03 |
| | **5% HA** | 154,2 ± 2,22 | 0,126 ± 0,04 |
| | **25% HA** | 159,7 ± 5,71 | 0,185 ± 0,02 |

***Table S2.*** *Size, PDI, charge, and encapsulation efficiency of DOTAP LNPs coated with 2% and 10% PSS.*

| LNP | Size (nm) | PDI | Zeta potential (mV) | Encapsulation efficiency (%) |
|---|---|---|---|---|
| **Control** | 152,8 ± 4,16 | 0,242 ± 0,03 | 13,5 ± 4,02 | 100,8 ± 0,12 |
| **5% HA** | 166,3 ± 1,55 | 0,148 ± 0,01 | -21,6 ± 0,88 | 102,0 ± 0,32 |
| **25% HA** | 163,1 ± 2,48 | 0,196 ± 0,02 | -17,7 ± 0,48 | 102,0 ± 0,37 |
| **2% PSS** | 132,8 ± 4,07 | 0,286 ± 0,04 | -34,6 ± 1,57 | 37,0 ± 10,31 |
| **10% PSS** | 154,1 ± 8,40 | 0,316 ± 0,04 | -41,7 ± 1,80 | -3,8 ± 2,83 |

***Table S3.*** *Size, PDI, charge, and encapsulation efficiency of DOTAP LNPs coated with 0.25% PSS.*

| LNP | Size (nm) | PDI | Zeta potential (mV) | Encapsulation efficiency (%) |
|---|---|---|---|---|
| **Control** | 202,7 ± 7,73 | 0,334 ± 0,03 | 13,2 ± 0,62 | 100,2 ± 0,15 |
| **5% HA** | 213,3 ± 18,00 | 0,340 ± 0,02 | -17,4 ± 1,03 | 99,5 ± 0,36 |
| **25% HA** | 231,7 ± 8,41 | 0,351 ± 0,03 | -20,6 ± 0,88 | 98,8 ± 0,43 |
| **0.25% PSS** | 157,6 ± 12,99 | 0,292 ± 0,04 | -12,4 ± 1,71 | 99,4 ± 0,41 |